

**Accelerated Article Preview****A vaccine targeting the RBD of the S protein of SARS-CoV-2 induces protective immunity**

Received: 17 March 2020

Accepted: 23 July 2020

Accelerated Article Preview Published  
online 29 July 2020

Cite this article as: Yang, J. et al. A vaccine targeting the RBD of the S protein of SARS-CoV-2 induces protective immunity. *Nature* <https://doi.org/10.1038/s41586-020-2599-8> (2020).

Jingyun Yang, Wei Wang, Zimin Chen, Shuaiyao Lu, Fanli Yang, Zhenfei Bi, Linlin Bao, Fei Mo, Xue Li, Yong Huang, Weiqi Hong, Yun Yang, Yuan Zhao, Fei Ye, Sheng Lin, Wei Deng, Hua Chen, Hong Lei, Ziqi Zhang, Min Luo, Hong Gao, Yue Zheng, Yanqiu Gong, Xiaohua Jiang, Yanfeng Xu, Qi Lv, Dan Li, Manni Wang, Fengdi Li, Shunyi Wang, Guanpeng Wang, Pin Yu, Yajin Qu, Li Yang, Hongxin Deng, Aiping Tong, Jiong Li, Zhenling Wang, Jinliang Yang, Guobo Shen, Zhiwei Zhao, Yuhua Li, Jingwen Luo, Hongqi Liu, Wenhai Yu, Mengli Yang, Jingwen Xu, Junbin Wang, Haiyan Li, Haixuan Wang, Dexuan Kuang, Panpan Lin, Zhengtao Hu, Wei Guo, Wei Cheng, Yanlin He, Xiangrong Song, Chong Chen, Zhihong Xue, Shaohua Yao, Lu Chen, Xuelei Ma, Siyuan Chen, Maling Gou, Weijin Huang, Youchun Wang, Changfa Fan, Zhixin Tian, Ming Shi, Fu-Sheng Wang, Lunzhi Dai, Min Wu, Gen Li, Guangyu Wang, Yong Peng, Zhiyong Qian, Canhua Huang, Johnson Yiu-Nam Lau, Zhenglin Yang, Yuquan Wei, Xiaobo Cen, Xiaozhong Peng, Chuan Qin, Kang Zhang, Guangwen Lu & Xiawei Wei

This is a PDF file of a peer-reviewed paper that has been accepted for publication. Although unedited, the content has been subjected to preliminary formatting. Nature is providing this early version of the typeset paper as a service to our authors and readers. The text and figures will undergo copyediting and a proof review before the paper is published in its final form. Please note that during the production process errors may be discovered which could affect the content, and all legal disclaimers apply.

# A vaccine targeting the RBD of the S protein of SARS-CoV-2 induces protective immunity

<https://doi.org/10.1038/s41586-020-2599-8>

Received: 17 March 2020

Accepted: 23 July 2020

Published online: 29 July 2020

Jingyun Yang<sup>1,13</sup>, Wei Wang<sup>1,13</sup>, Zimin Chen<sup>1,13</sup>, Shuaiyao Lu<sup>3,13</sup>, Fanli Yang<sup>1,13</sup>, Zhenfei Bi<sup>1,13</sup>, Linlin Bao<sup>4,13</sup>, Fei Mo<sup>1</sup>, Xue Li<sup>1</sup>, Yong Huang<sup>1</sup>, Weiqi Hong<sup>1</sup>, Yun Yang<sup>3</sup>, Yuan Zhao<sup>3</sup>, Fei Ye<sup>1</sup>, Sheng Lin<sup>1</sup>, Wei Deng<sup>4</sup>, Hua Chen<sup>1</sup>, Hong Lei<sup>1</sup>, Ziqi Zhang<sup>1</sup>, Min Luo<sup>1</sup>, Hong Gao<sup>4</sup>, Yue Zheng<sup>1</sup>, Yanqiu Gong<sup>1</sup>, Xiaohua Jiang<sup>1</sup>, Yanfeng Xu<sup>4</sup>, Qi Lv<sup>4</sup>, Dan Li<sup>1</sup>, Manni Wang<sup>1</sup>, Fengdi Li<sup>4</sup>, Shunyi Wang<sup>4</sup>, Guanpeng Wang<sup>4</sup>, Pin Yu<sup>4</sup>, Yajin Qu<sup>4</sup>, Li Yang<sup>1</sup>, Hongxin Deng<sup>1</sup>, Aiping Tong<sup>1</sup>, Jiong Li<sup>1</sup>, Zhenling Wang<sup>1</sup>, Jinliang Yang<sup>1</sup>, Guobo Shen<sup>1</sup>, Zhiwei Zhao<sup>1</sup>, Yuhua Li<sup>5</sup>, Jingwen Luo<sup>1</sup>, Hongqi Liu<sup>3</sup>, Wenhai Yu<sup>3</sup>, Mengli Yang<sup>3</sup>, Jingwen Xu<sup>3</sup>, Junbin Wang<sup>3</sup>, Haiyan Li<sup>3</sup>, Haixuan Wang<sup>3</sup>, Dexuan Kuang<sup>3</sup>, Panpan Lin<sup>1</sup>, Zhengtao Hu<sup>7</sup>, Wei Guo<sup>7</sup>, Wei Cheng<sup>1</sup>, Yanlin He<sup>7</sup>, Xiangrong Song<sup>1</sup>, Chong Chen<sup>1</sup>, Zhihong Xue<sup>1</sup>, Shaohua Yao<sup>1</sup>, Lu Chen<sup>1</sup>, Xuelei Ma<sup>1</sup>, Siyuan Chen<sup>1</sup>, Maling Gou<sup>1</sup>, Weijin Huang<sup>5</sup>, Youchun Wang<sup>5</sup>, Changfa Fan<sup>5</sup>, Zhixin Tian<sup>6</sup>, Ming Shi<sup>8</sup>, Fu-Sheng Wang<sup>8</sup>, Lunzhi Dai<sup>1</sup>, Min Wu<sup>1</sup>, Gen Li<sup>11</sup>, Guangyu Wang<sup>12</sup>, Yong Peng<sup>1</sup>, Zhiyong Qian<sup>1</sup>, Canhua Huang<sup>1</sup>, Johnson Yiu-Nam Lau<sup>9</sup>, Zhenglin Yang<sup>10</sup>, Yuquan Wei<sup>1</sup>, Xiaobo Cen<sup>1,7</sup>, Xiaozhong Peng<sup>3</sup>, Chuan Qin<sup>4</sup>, Kang Zhang<sup>11,13</sup>, Guangwen Lu<sup>1,2,13</sup> & Xiawei Wei<sup>1,13</sup>

The novel Coronavirus SARS-CoV-2 causes a respiratory illness called COVID-19 leading to a pandemic. An effective preventive vaccine against this virus is urgently needed. As the most critical step during infection, SARS-CoV-2 uses its Spike protein receptor-binding domain (S-RBD) to engage with the host cell receptor angiotensin-converting enzyme 2 (ACE2)<sup>1,2</sup>. Here we showed that a recombinant vaccine comprising residues 319-545 of the S-RBD could induce a potent functional antibody response in the immunized mice, rabbits and non-human primates (*Macaca mulatta*) as early as 7 or 14 days after a single dose injection. The sera from the immunized animals blocked RBD binding to ACE2 expressed on the cell surface and neutralized the infection by SARS-CoV-2 pseudovirus and live SARS-CoV-2 *in vitro*. Importantly, the vaccination also provided protection in non-human primates from SARS-CoV-2 challenge *in vivo*. The elevated RBD-specific antibodies were also found in the sera from patients with COVID-19. Several immune pathways and CD4 T lymphocytes were implicated in the induction of the vaccine antibody response. Our finding highlights the importance of the RBD domain in the SARS-CoV-2 vaccine design and provides the rationale for the development of a protective vaccine through the induction of antibody against the RBD domain.

The novel Coronavirus SARS-CoV-2, which causes a respiratory illness called COVID-19, has been declared as a pandemic by the World Health Organization. Person-to-person transmission has been documented<sup>3,4</sup>. There is an urgent need for an effective preventive vaccine.

SARS-CoV-2 binds to cells utilizing the human angiotensin-converting enzyme 2 (ACE2) as a receptor<sup>1,2</sup>. Based on our knowledge of the viral envelope protein, we hypothesized that the receptor binding domain (RBD) will be a good immunogen and can trigger a potent functional

<sup>1</sup>Laboratory of Aging Research and Cancer Drug Target, State Key Laboratory of Biotherapy and Cancer Center, National Clinical Research Center for Geriatrics, West China Hospital, Sichuan University, Sichuan, 610041, People's Republic of China. <sup>2</sup>Emergency Department, State Key Laboratory of Biotherapy, West China Hospital, Sichuan University, Sichuan, People's Republic of China. <sup>3</sup>National Kunming High-level Biosafety Primate Research Center, Institute of Medical Biology, Chinese Academy of Medical Sciences and Peking Union Medical College, Yunnan China and State Key Laboratory of Medical Molecular Biology, Chinese Academy of Medical Sciences, School of Basic Medicine Peking Union Medical College, Beijing, China. <sup>4</sup>Key Laboratory of Human Disease Comparative Medicine, Chinese Ministry of Health, Beijing Key Laboratory for Animal Models of Emerging and Reemerging Infectious Diseases, Institute of Laboratory Animal Science, Chinese Academy of Medical Sciences and Comparative Medicine Center, Peking Union Medical College, Beijing, China. <sup>5</sup>National Institutes for Food and Drug Control (NIFDC), Beijing, 102629, China. <sup>6</sup>School of Chemical Science & Engineering and Shanghai Key Laboratory of Chemical Assessment and Sustainability, Tongji University, Shanghai, 200092, China. <sup>7</sup>National Chengdu Center for Safety Evaluation of Drugs, State Key Laboratory of Biotherapy and Cancer Center, West China Hospital, Sichuan University, and Collaborative Innovation Center for Biotherapy, Chengdu, 610041, China. <sup>8</sup>Treatment and Research Center for Infectious Diseases, The Fifth Medical Center of PLA General Hospital, National Clinical Research Center for Infectious Diseases, Beijing, 100039, China. <sup>9</sup>Department of Applied Biology and Chemical Technology, Hong Kong Polytechnic University, Hung Hom, Hong Kong. <sup>10</sup>Sichuan Provincial Key Laboratory for Human Disease Gene Study and Institute of Laboratory Medicine, Sichuan Provincial People's Hospital, University of Electronic Science and Technology of China, Chengdu, Sichuan, 610072, China. <sup>11</sup>Center for Biomedicine and Innovations at Faculty of Medicine, Macau University of Science and Technology, Macau, China. <sup>12</sup>Department of Computer Science and Technology, Tsinghua University, Beijing, China. <sup>13</sup>These authors contributed equally: Jingyun Yang, Wei Wang, Zimin Chen, Shuaiyao Lu, Fanli Yang, Zhenfei Bi, Linlin Bao.

✉e-mail: kang.zhang@gmail.com; lugw@scu.edu.cn; xiaweiwei@scu.edu.cn

antibody response that can neutralize SARS-CoV-2 *in vitro* and in a SARS-CoV-2 infection model in non-human primates (*Macaca mulatta*) *in vivo* through the blocking of viral envelope to its host cell receptor ACE2.

The baculovirus expression system was chosen to express the various proteins for our study as this is a commercially feasible system and can manufacture the candidate vaccine, if successful, in a commercial scale, and the vaccine generated are in general with correctly folded protein conformation<sup>5,6</sup>. In fact, this technology was used in several commonly used vaccine products, including some of the cervical cancer vaccine and influenza vaccines currently in the European and the United States markets<sup>5,6</sup>. The objective of this study was to evaluate the potential of a candidate vaccine based on the RBD domain of SARS-CoV-2, to evaluate the appropriate dosing regime and to test its effect in generating neutralizing activity against SARS-CoV-2 in the recipient animals, and determine the immune pathways involved in the generation of the immune response, so as to provide the groundwork for the design of an effective SARS-CoV-2 preventive vaccine.

### Characterization of the recombinant SARS-CoV-2 S RBD protein

The recombinant receptor-binding domain (RBD) protein of SARS-CoV-2 spike protein was prepared using insect cells and the Bac-to-Bac Baculovirus Expression System as described previously<sup>7,8</sup>. A GP67 signal peptide sequence was added to ensure protein secretion (Figure 1a). Recombinant RBD was successfully harvested from the culture supernatant and purified to high homogeneity. The purity of the final protein preparation was over 98% (Figure 1b).

The apparent molecular weight of the purified RBD protein was determined to be 34 kDa, which was approximately 1/4 larger than that calculated from the molecular weight of the RBD amino acid sequence alone (about 27 kDa), suggesting dense protein glycosylation. Via mass spectrometry (MS), the intact N-glycopeptides and glycans were analyzed using the GPSeeker software<sup>8,9</sup>. Three N-glycosylation sites on asparagine were identified (Figure 1c). The O-glycosylation sites were also evaluated by analyzing the MS results using SEQUEST in Proteome Discoverer (version 2.3). Some well-known O-linked glycans such as HexNAc and Hex(1)HexNAc(1) were searched as potential variable modifications<sup>9,10</sup>. In total, ten O-glycosylation sites were identified (Figure 1c). To determine the abundance of glycosylation, the number of MS/MS spectra of glycosylated peptides and their corresponding unmodified peptides were both determined. A much higher degree of N-glycosylation than O-glycosylation was observed (Figure 1d).

These identified glycosylation sites were further mapped on the complex structure of SARS-CoV-2 RBD bound to ACE2. A majority of the sites were located on the RBD core subdomain (Figure 1e). In addition, all the sites were found to be distant from the bound ACE2 (Figure 1e), indicating that the decorated glycans may not interfere with receptor recognition/binding.

The binding of our RBD protein with ACE2 was then confirmed via surface plasmon resonance Biacore. In concordance with a previous study<sup>2</sup>, potent interactions were observed. The binding affinity was calculated to be about 1.54 nM in dissociation constant ( $K_D$ ), with  $k_a$  of  $1.33 \times 10^7 \text{ M}^{-1} \text{ S}^{-1}$  and  $k_d$  of  $2.05 \times 10^2 \text{ S}^{-1}$  (Figure 1f). This finding showed that our RBD binds to ACE2 with a high affinity, which is a good reflection of the native conformation for our RBD protein.

### Identification of serum antibody against S protein RBD in patients and animal models

First, alum-precipitation was selected to serve as a vaccine adjuvant based on its long record of effectiveness and safety<sup>11,12</sup>. In this study, all vaccine preparations were prepared by the addition of aluminum

hydroxide gel to various proteins, resulting in alum-precipitated protein vaccine candidates.

Mice were immunized with different dose range (0.1 to 20  $\mu\text{g}$ ) and regimen. For example, mice were immunized with a single injection on Day 0 and collected sera on day 7; or with two vaccinations on day 0, day 7 and collected sera on day 21, with two doses on day 0, day 14 and sera collected on day 21. In some experiments, a third dose on Day 21 was also given. To assess the humoral immune responses induced by the recombinant RBD, enzyme-linked immunosorbent assay (ELISA) for RBD-specific antibodies was employed. Given the urgent need of an effective vaccine globally, special attention was provided to the early antibody response and its ability to neutralize SARS-CoV-2.

Sera obtained on day 7 after the first dose of the candidate vaccine already showed elevated IgG and IgM responses to the recombinant RBD (Figure 2a). In contrast, the sera from pre-immunization and those from PBS and Alum gel controls had only background-level antibody responses. Furthermore, the antibody reaction was dose-dependent, and could be induced with a very low dose of the vaccinated protein (0.1  $\mu\text{g}/\text{mice}$ ) 7 days after the administration (Figure 2b). The recombinant RBD protein alone was already effective in inducing specific antibodies production, but the addition of the Alum adjuvant could significantly enhance the induction with a higher level of specific antibodies by day 7 (Figure 2a) and even more by day 21 (Figure 2c). The sera obtained 9 days after the third vaccination (booster dose given on day 21) showed a very strong specific antibody response in the mice (Figure 2d), with a positive reaction at a dilution of 1:204,800.

The antibody reaction was also dose-dependent (Figure 2b). The dose-dependent response was also observed in rabbits, and a good level of specific antibody could be induced with a low dose at 1  $\mu\text{g}/\text{rabbit}$  per injection and with three doses of the candidate vaccines given ( $n=40$  rabbits, Extended Data Figure 1a). Importantly, we also tested the viral neutralization activity of the sera as challenged *in vitro* with a pseudovirus and a high level of activity was observed (see below, and Extended Figure 1b).

We also tested our candidate vaccine in non-human primates (*Macaca mulatta*). Ten monkeys were vaccinated at day 0 and Day 7 and immune sera were obtained at day 7 after each vaccination with our candidate vaccine or pre-immunization was used as a reference. Sera at day 7 and 14 post-immunization showed a significantly elevated IgG response to the recombinant RBD and had an increased level of neutralizing antibodies against pseudovirus (Extended Data Figure 1). Also, the neutralizing antibodies against live SARS-CoV-2 was demonstrated in the vaccination of non-human primates and challenge with live SARS-CoV-2 (see below, Figure 3 c).

The antigenicity of the recombinant RBD was also tested for seroreactivity in sera obtained from healthy human subjects and patients with COVID-19. Sera from 20 healthy donors and 16 patients with COVID-19 were tested for their IgG and IgM responses to the recombinant RBD. All 16 COVID19 patients showed significant elevated levels of IgG and IgM against the recombinant RBD, compared with the background signal recorded in the healthy donors (Figure 2e).

### Functional characterization of the sera from the immunized animals and the prevention of the non-human primates (*Macaca mulatta*) from SARS-CoV-2 infection

In the next sets of experiments, sera from the immunized animals were tested for its blocking activity of RBD to ACE2 receptor. Negative control Huh7 cells in the absence of immune sera had RBD-ACE2-positivity detected in 90.2% of cells (Figure 3a). With the immunized sera obtained in mice 7 days after one dose (5  $\mu\text{g}$ ) of the candidate vaccine, only 14.3% Huh7 cells were RBD-ACE2 positive. Sera from the mice treated with phosphate buffered saline (PBS) at the same dilution had nearly no inhibitory activity with 87.4% ACE2 positive cells (Figure 3a).

These findings indicated that the sera from the early vaccination with a single dose (5 µg) in mice could effectively block RBD binding to AEC2 receptor on the cells.

A neutralization assay using pseudovirus is regarded as a sensitive and quantitative method for SARS-CoV and MERS-CoV<sup>13</sup>. Immune sera from the non-human primates (*Macaca mulatta*), mice and rabbits were tested for the neutralizing activity against SARS-CoV-2 pseudovirus in 293T cells expressing ACE2. Immune sera from the non-human primates (*Macaca mulatta*) 7 days after the first vaccination can block the infection by SARS-CoV-2 pseudovirus near completely (Figure 3b). Similarly, near complete neutralization of SARS-CoV-2 pseudovirus was observed using the immune sera from mice and rabbits 14 days after the first vaccination (Extended Data Figure 3a and b). In addition, the immune sera from both human ACE2 transgenic mice and wild type mice 14 days after the second vaccination showed a similar level of the neutralizing antibodies with a calculated dilution of 1: 32 or lower that can completely protect Vero E6 cells from live SARS-CoV-2 infection (Extended Data Figure 4). When the immune sera from rabbits immunized with three doses of the vaccine candidate were tested, a viral neutralization activity with an EC50 at a calculated dilution of 1: 2826 was observed in rabbits (Extended Data Figure 1b).

In the next experiments, we also tested whether the RBD vaccine could block the infection in non-human primates inoculated with live SARS-CoV-2. We immunized non-human primates (*Macaca mulatta*) with two injections on day 0, day 7 via the intramuscular route with 20 µg or 40 µg per dose and then challenged with live SARS-CoV-2 viruses 28 days after the first vaccination. The control groups included the treatment with PBS or aluminum hydroxide gel alone. Neutralizing antibodies against live SARS-CoV-2 were detected in all vaccinated non-human primates, whereas no neutralizing antibodies were detected in the two control groups (Figure 3c).

A quantitative real-time reverse transcription-PCR (qRT-PCR) was employed to measure viral genomic RNA (gRNA) and viral subgenomic RNA (sgRNA, indicative of viral replication). Lung tissues of non-human primates were collected on day 7 following challenge to determine the viral replication status. Lung tissues from the control groups showed excessive copies of the viral gRNA and sgRNA in lung tissues. In contrast, no detectable viral gRNA or viral sgRNA was present in the vaccinated groups with 20 µg and 40 µg of the vaccine with adjuvant given (Figure 3d). In addition, peak loads of viral gRNA in the throat swabs were observed in the controls (Figure 3e) 3 days post inoculation (DPI) and these were blocked by the vaccination, with only ~1.6 and 3.8 parts per million of the viral loads in the vaccinated groups with 20 and 40 µg of vaccines given, respectively, compared with those of the control group. Importantly, no detectable sgRNA in the throat swabs was observed in the vaccinated groups with both 20 µg and 40 µg doses after the challenge (Figure 3e), whereas high levels of sgRNA, indicative of viral replication, was observed in the control groups. Peak levels of viral gRNA and sgRNA in the anal swabs were observed in the control groups at 5- and 6-days post inoculation, but only a very low level detection in the vaccinated groups and again no detectable sgRNA was detected in the anal swabs in the vaccinated non-human primates in both 20 and 40 µg dose groups (Figure 3f). These data were consistent that the low gRNA detected was from the high inoculation dose which might be neutralized already and there was no evidence of viral replication as reflected by the absence of detectable sgRNA.

The lung tissues from the two control groups (aluminum hydroxide or PBS alone) revealed typical histopathological changes of viral interstitial pneumonia, a key feature of COVID-19. As shown in Figure 3g, the microscopic findings included apparent thickened alveolar walls, heavy interstitial mononuclear inflammatory cell infiltrates. The alveolar space also exhibited a heavy infiltration and exudates with the disappearance of recognizable architecture. In addition, diffuse hemorrhage and Type II pneumocyte hyperplasia was also observed. In contrast, non-human primates vaccinated with the RBD vaccine (20 µg or 40 µg)

exhibited no significant histopathological changes, with the appearance of the normal lung tissues (Figure 3g).

### Assessment of the immune cellular pathways involved with the RBD vaccination

Next, the potential pathways through which our recombinant RBD protein vaccine was involved in mounting this immune humoral response were evaluated. As shown in Extended Data Figure 5a, the mice deficient in *Cd4<sup>-/-</sup>*, *Sting1<sup>-/-</sup>*, *Casp1<sup>-/-</sup>*, *Nlrp3<sup>-/-</sup>*, *Il-1β<sup>-/-</sup>*, *Tlr2<sup>-/-</sup>*, and *Tlr4<sup>-/-</sup>* showed reduction in the level of IgG induced against the RBD protein, as compared to wild-type mice, while others (*Cd8a<sup>-/-</sup>* mice) showed no effect on the level of IgG induction.

Cellular immune responses may be also involved in the clearance of SARS-CoV infection in which both CD4 and CD8 T cells are involved<sup>14-16</sup>. The lymphocytes isolated from the candidate vaccine-immunized mice induced elevated levels of IFN-γ and IL-4 when stimulated with recombinant RBD (Extended Data Figure 5b). Moreover, using flow cytometry, the number of the memory lymphocytes, CD4+CD44<sup>high</sup>+IL-4+, CD4+CD44<sup>high</sup>+IFN-γ, CD8+CD44<sup>high</sup>+IFN-γ, were found to be increased in the candidate RBD vaccinated-mice (Extended Data Figure 5c).

In order to investigate whether immune sera versus splenic T cells triggered by our vaccine play a role in the protection from live SARS-CoV-2, we performed adoptive therapy of immune sera versus splenic T cells from the vaccinated mice. Adoptive therapy of splenic T cells (CD4+ and CD8+ cells) did not provide the protection from the infection of SARS-CoV-2. By contrast, at the same time, adoptive therapy of 0.1 ml of the pooled sera from the immunized mice showed no detectable viral replication (Figure 4a), no significant histopathological changes (Extended Data Figure 6a) as well as no weight loss (Extended Data Figure 6b), compared with those from the mice treated with PBS as a control. Even the sera from mice 7 days after a single dose of the vaccine can completely prevent mice from the infection with live SARS-CoV-2 (Extended Data Figure 6c-e). In addition, no evidence of antibody-dependent enhancement or acceleration of pneumonia was observed as no mice that received the RBD-vaccinated immune sera developed any evidence of pneumonia. In consideration of the important role of the antibody for the protective immunity in the present study, we also test the other forms of the spike-protein for the optimal induction of the neutralizing antibodies, and found that the recombinant RBD protein vaccine had a much higher viral neutralization activity with an EC50 compared with the extracellular domain protein (ECD), S1-subunit protein (S1) (Figure 4b). No viral neutralization activity was found with S2-subunit protein (S2) vaccine.

Although elevated levels of INF-γ and IL-4 was observed to be produced by the lymphocytes stimulated by the RBD *in vitro*, there were no significant increase in any of these two and other inflammatory cytokines in the plasma in these mice (Extended Data Figure 5d), indicating that the RBD did not induced a systemic inflammatory reaction.

To further address the safety of the candidate vaccine, the potential toxicity of the vaccine was evaluated in the non-human primates (n=50) in compliance with Good Laboratory Practices (GLP). No adverse events were observed including body weight, ruffling of fur, behavioral changes, appetite, etc. No pathologic changes were observed in liver, lung, kidney, spleen, brain, heart, or other tissues on microscopic examination. No changes in peripheral blood counts and differentials were noted (data not shown).

### Discussion

SARS-CoV-2 is causing a major pandemic and an effective vaccine is urgently needed. It has been reported that several vaccines including inactivated viruses, adenoviral vectors carrying S protein or RNA vaccines have been tested in monkeys or in clinical trials<sup>17-20</sup>. The fact



that our candidate RBD vaccine can induce effective a viral neutralizing activity in three different animal species, rodents, rabbits, and non-human primates is very encouraging. It is also encouraging to observe (a) that the antibodies shared common binding epitopes from infected patients, (b) that there is a strong viral neutralizing activity associated with a good humoral response, (c) that a simple vaccine adjuvant like Alum can further enhance the immune response, (d) that even one dose of the vaccine can already generated an excellent level of viral neutralizing activity, (e) that the vaccine can protect non-human primates from live SARS-CoV-2 challenge, and (f) that the toxicology studies in the non-human primates showed that this vaccine candidate is safe. Also, our vaccine strategy based on RBD has been supported by the recent findings that the majority of the neutralizing activity is directed towards RBD in the sera of COVID-19 patients and by human monoclonal antibodies<sup>20–22</sup>. In addition, this recombinant RBD approach may be technically and commercially feasible to manufacture at a massive global supply scale. All these features are excellent prospects in supporting the further development of this vaccine candidate.

What was also intriguing was the early protective viral neutralizing activity observed. Given the current pandemic, developing some type of viral neutralizing activity around 7 days after the first dose would be very helpful (while still following the final vaccination regime as defined clinically), this effect may have tremendous impact on treating infected individuals and preventing the spread of SARS-COV-2 in the populations. Although we found no evidence of enhancement in the passive transfer model in mice or upon viral challenge of the immunized non-human primates, this does not rule out the possibility of the enhancement by antibodies or cellular immunity after vaccination in other species including humans.

In summary, our finding highlights the importance of the RBD domain in S protein in the SARS-CoV-2 vaccine design and provides the rationale for the development of a protective vaccine through the induction of antibodies against RBD domain.

## Online content

Any methods, additional references, Nature Research reporting summaries, source data, extended data, supplementary information, acknowledgements, peer review information; details of author contributions and competing interests; and statements of data and code availability are available at <https://doi.org/10.1038/s41586-020-2599-8>.

- Zhou, P. et al. A pneumonia outbreak associated with a new coronavirus of probable bat origin. *Nature* **579**, 270–273 (2020).
- Wrapp, D. et al. Cryo-EM structure of the 2019-nCoV spike in the prefusion conformation. *Science* **367**, 1260–1263 (2020).
- Li, Q. et al. Early Transmission Dynamics in Wuhan, China, of Novel Coronavirus-Infected Pneumonia. *N. Engl. J. Med.* **382**, 1199–1207 (2020).
- Huang, C. et al. Clinical features of patients infected with 2019 novel coronavirus in Wuhan, China. *Lancet* **395**, 497–506 (2020).
- Contreras-Gómez, A., Sánchez-Mirón, A., García-Camacho, F., Molina-Grima, E. & Chisti, Y. Protein production using the baculovirus-insect cell expression system. *Biotechnology progress* **30**, 1–18 (2014).
- Cox, M. M. & Hashimoto, Y. A fast track influenza virus vaccine produced in insect cells. *Journal of invertebrate pathology* **107**, S31–S41 (2011).
- Lu, G. et al. Molecular basis of binding between novel human coronavirus MERS-CoV and its receptor CD26. *Nature* **500**, 227–231 (2013).
- Wang, Q. et al. Bat origins of MERS-CoV supported by bat coronavirus HKU4 usage of human receptor CD26. *Cell host & microbe* **16**, 328–337 (2014).
- Xiao, K. & Tian, Z. GPSeeker Enables Quantitative Structural N-Glycoproteomics for Site- and Structure-Specific Characterization of Differentially Expressed N-Glycosylation in Hepatocellular Carcinoma. *Journal of proteome research* **18**, 2885–2895 (2019).
- Wang, Y., Xu, F., Xiao, K., Chen, Y. & Tian, Z. Site- and structure-specific characterization of N-glycoprotein markers of MCF-7 cancer stem cells using isotopic-labelling quantitative N-glycoproteomics. *Chem. Commun. (Camb.)* **55**, 7934–7937 (2019).
- MacLeod, M. K. et al. Vaccine adjuvants aluminum and monophosphoryl lipid A provide distinct signals to generate protective cytotoxic memory CD8 T cells. *Proceedings of the National Academy of Sciences of the United States of America* **108**, 7914–7919 (2011).
- Luo, M. et al. Simultaneous enhancement of cellular and humoral immunity by the high salt formulation of Al(OH)<sub>3</sub> adjuvant. *Cell research* **27**, 586–589 (2017).
- Wong, S. K., Li, W., Moore, M. J., Choe, H. & Farzan, M. A 193-amino acid fragment of the SARS coronavirus S protein efficiently binds angiotensin-converting enzyme 2. *The Journal of biological chemistry* **279**, 3197–3201 (2004).
- Yang, Z. Y. et al. A DNA vaccine induces SARS coronavirus neutralization and protective immunity in mice. *Nature* **428**, 561–564 (2004).
- Guo, Y. et al. Elicitation of immunity in mice after immunization with the S2 subunit of the severe acute respiratory syndrome coronavirus. *DNA Cell Biol.* **24**, 510–515 (2005).
- He, Y. et al. Cross-neutralization of human and palm civet severe acute respiratory syndrome coronaviruses by antibodies targeting the receptor-binding domain of spike protein. *J Immunol* **176**, 6085–6092 (2006).
- van Doremalen, N. et al. ChAdOx1 nCoV-19 vaccination prevents SARS-CoV-2 pneumonia in rhesus macaques. *bioRxiv* (2020).
- Zhu, F. C. et al. Safety, tolerability, and immunogenicity of a recombinant adenovirus type-5 vectored COVID-19 vaccine: a dose-escalation, open-label, non-randomised, first-in-human trial. *Lancet* **395**, 1845–1854 (2020).
- Gao, Q. et al. Rapid development of an inactivated vaccine candidate for SARS-CoV-2. *Science* (2020).
- Dai, L. et al. A universal design of betacoronavirus vaccines against COVID-19, MERS and SARS. *Cell* (2020).
- Robbiani, D. F. et al. Convergent antibody responses to SARS-CoV-2 in convalescent individuals. *Nature* (2020).
- Wec, A. Z. et al. Broad neutralization of SARS-related viruses by human monoclonal antibodies. *Science* (2020).

**Publisher's note** Springer Nature remains neutral with regard to jurisdictional claims in published maps and institutional affiliations.

© The Author(s), under exclusive licence to Springer Nature Limited 2020

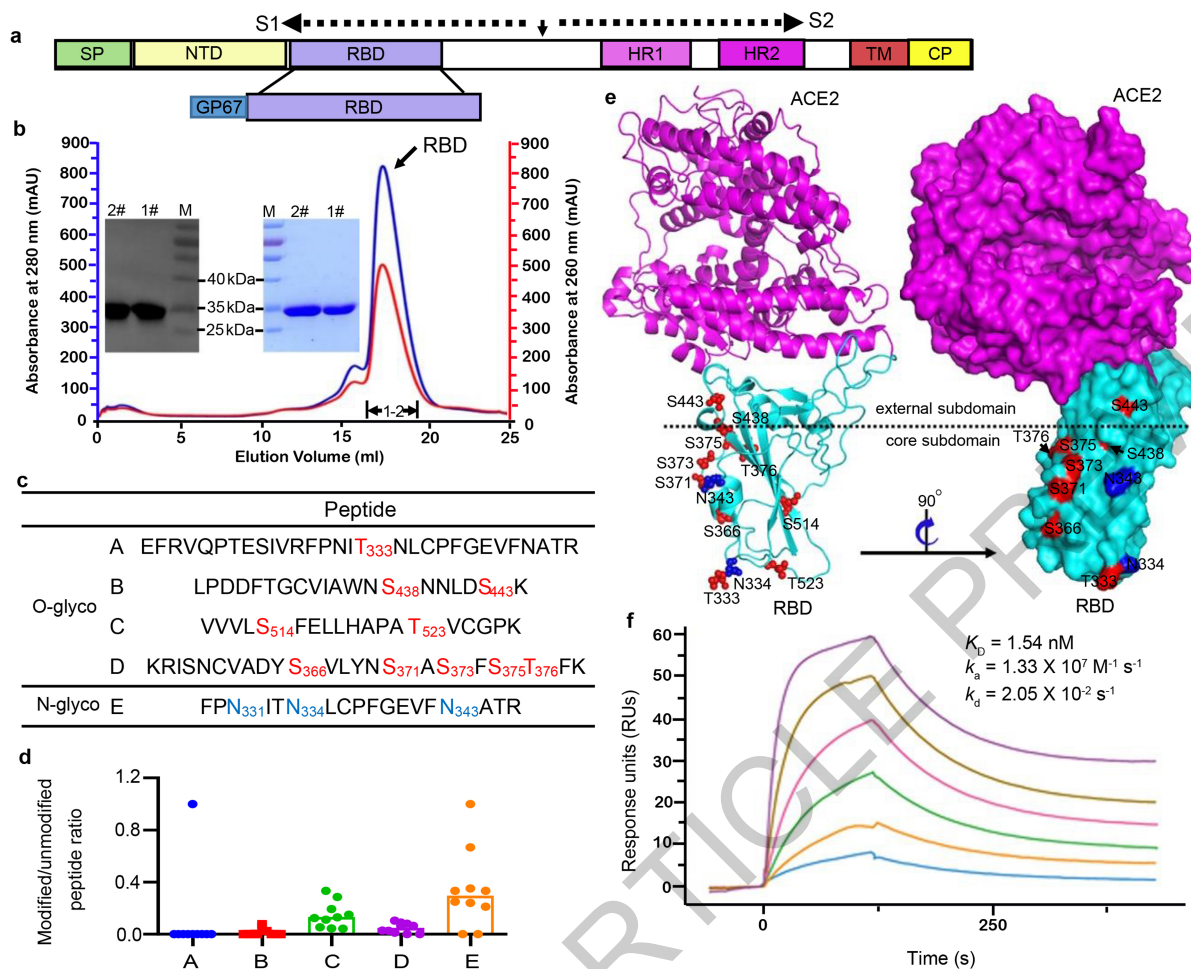


**Fig. 1 | Characterization of the SARS-CoV-2 S RBD protein.** **a.** A schematic view of the SARS-CoV-2 S protein. The indicated domains and elements, including signal peptide (SP), N-terminal domain (NTD), receptor binding domain (RBD), heptad repeat 1 and 2 (HR1 and HR2), transmembrane domain (TM) and cytoplasmic domain (CP), are marked. For S RBD preparation, the RBD region was engineered to include an N-terminal GP67 signal peptide. **b.** A representative elution chromatograph of the recombinant RBD protein on a Superdex 200 increase column. The inset figures showed the SDS-PAGE and western-blotting analyses of the eluted RBD samples. **c.** Glycosylated peptides in RBD identified by mass spectrometry. The N-glycosylation and O-glycosylation sites are marked with the residue numbers. **d.** The abundance of glycosylation. The number of MS/MS spectra of each glycosylated peptides listed in **c** and their corresponding

unmodified peptides were counted. Nine sample preparation and MS acquisition methods are applied. Each spot means the results from one method. **e.** An overview of the glycosylation sites illustrated based on the solved complex structure of SARS-CoV-2 RBD bound to ACE2 (PDB code: 6LZG). The identified sites, colored red for O-glycosylation and blue for N-glycosylation, are shown as spheres and labeled. The approximate boundary between the core and external subdomains in RBD are marked with a dashed line. The right panel (surface representation) was generated by rotating the structure in the left panel (cartoon representation) around a vertical axis for about 90°. **f.** The real-time binding profile between our purified RBD protein and ACE2 characterized by SPR Biacore.

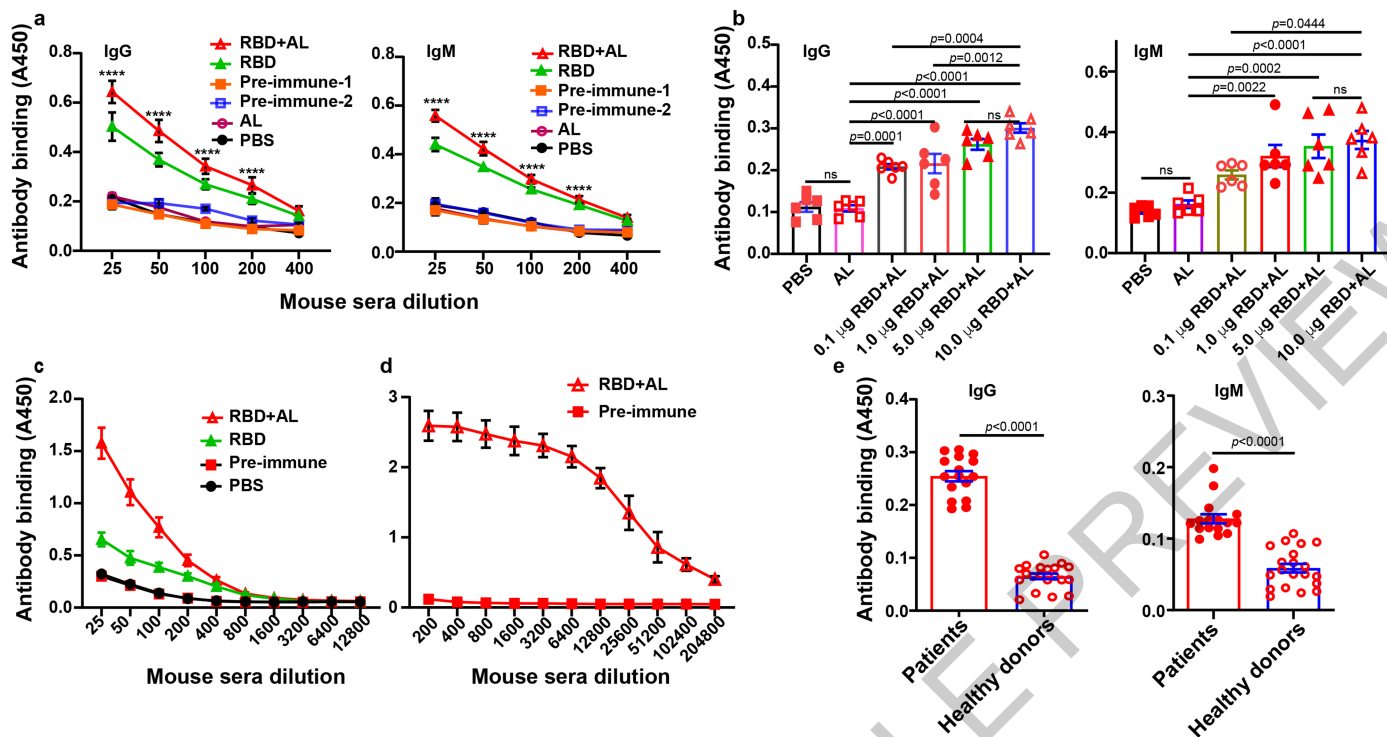


**Fig. 2 | Serum antibody response against S protein RBD in patients and in mice as determined by ELISA.** **a.** The mice were immunized with 5 µg recombinant RBD protein per mouse in 50 µl in the presence of aluminum hydroxide, compared with the control groups including recombinant RBD protein alone, with aluminum hydroxide (AL), pre-immune or PBS alone. Sera were collected from the mice 7 days after the first dose of vaccine and were tested with different dilution for IgG and IgM against recombinant RBD protein using ELISA as described in Methods. Data are presented as mean±SEM of five mouse sera in each group. P-values were determined by two-way ANOVA. P-values indicated RBD+AL vs AL or PBS or pre-immune groups. RBD+AL vs RBD alone in IgG level:  $P < 0.0001$  and  $P < 0.002$  at dilution of 1:25 and 1:50 respectively. AL:  $Al(OH)_3$ , RBD: recombinant RBD protein, RBD+AL: the addition of the recombinant RBD protein to  $Al(OH)_3$ , PBS – phosphate buffered saline. Similar results were repeated in three independent experiments. **b.** The mice were immunized with 0.1-10 µg recombinant RBD protein per mouse in

50 µl in the presence of AL, or AL alone or PBS alone. Sera were collected from the mice 7 days after the first dose of vaccine and were tested at 1:50 dilution for IgG and IgM against S protein RBD using ELISA. Data were presented as mean±SEM of six mouse serum samples in each group. P-values were determined by one-way ANOVA. **c.** Sera were collected 14 days after two vaccinations on day 0 and day 7 with 5 µg recombinant RBD protein per mouse in 50 µl in the presence of aluminum hydroxide, or recombinant RBD protein alone, and the level of the IgG of the sera was tested at the different dilution by ELISA. Similar results were repeated in three independent experiments. **d.** Sera were collected from 9 days after the three vaccinations on day 0, day 14 and day 21 with the same doses as **c.** **e.** Serum samples were collected from 16 patients infected with SARS-CoV-2 (and recovered) and 20 healthy donors and detected with 1:5 diluted sera with ELISA as described in Methods. Data are presented as the mean±SEM. P-values were determined by one-way ANOVA.

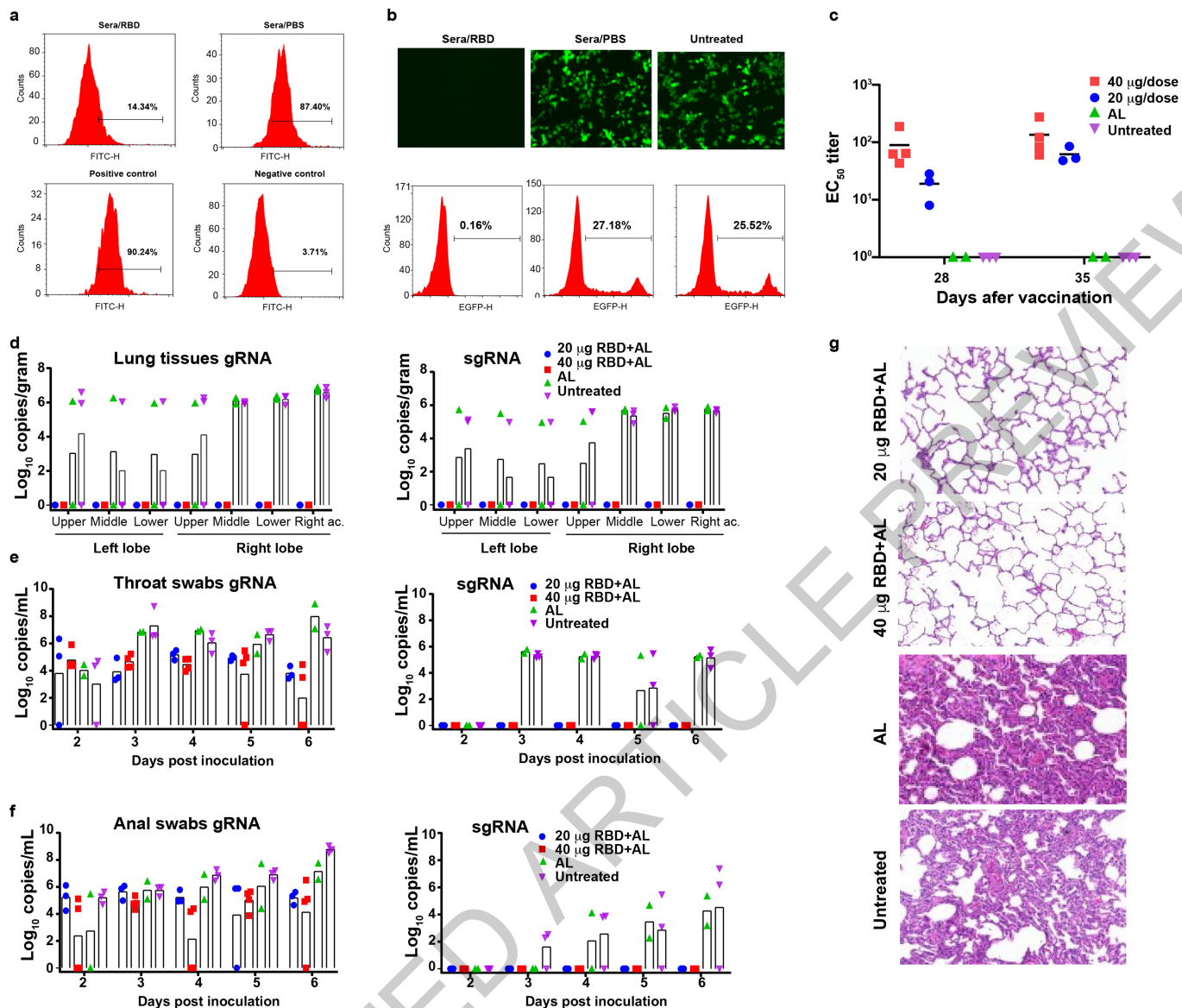


**Fig. 3 | Functional characterization of the sera from the immunized animals and the protection of the Non-human primates, *Macaca mulatta*, from SARS-CoV-2 infection.** **a.** Inhibition of the S protein RBD binding to cell-surface ACE2. Recombinant SARS-CoV-2 RBD-Fc fusion protein was added to ACE2-positive Huh7 cells in the presence or absence of the sera at a dilution of 1:5, followed by incubating with anti-human IgG-FITC conjugate. Sera/RBD (sera from the mice immunized with RBD vaccine day 7 after the first vaccination), Sera/PBS (from the mice treated by PBS as a control), Positive control (without Sera/RBD or Sera/PBS), Negative control (stained with anti-human IgG-FITC conjugate alone). **b.** The neutralization of SARS-CoV-2 pseudovirus infection by the sera from non-human primates. Sera/RBD (sera from the non-human primates immunized with RBD) and Sera/PBS (sera from those treated by PBS as a control), Untreated (infection with SARS-CoV-2 pseudovirus without sera). **c-g.**

Non-human primates (*Macaca mulatta*) were immunized with two injections on day 0, day 7 via the intramuscular route with 20 µg or 40 µg per dose and then challenged with SARS-CoV-2 intranasally (0.5 ml, 10<sup>6</sup> pfu/ml) on day 28 after the first vaccination as described in methods. **c.** Neutralization of live SARS-CoV-2 infection by the immune sera from non-human primates was measured as described in Methods. A quantitative real-time reverse transcription-PCR (qRT-PCR) was employed to measure viral genomic RNA (gRNA) and viral subgenomic RNA (sgRNA, indicative of virus replication) in lung tissues (**d**), the throat swabs (**e**), and the anal swabs (**f**). Pictured are individual values with geometric mean bars. 40 µg RBD+AL: vaccinated with 40 µg recombinant RBD protein with Al(OH)<sub>3</sub> (n=4); 20 µg RBD+AL: 20 µg recombinant RBD protein with Al(OH)<sub>3</sub> (n=3); Untreated: treated with PBS (n=3), AL: Al(OH)<sub>3</sub> alone (n=2). **g.** Histopathological changes in lung tissues observed by light microscopy.

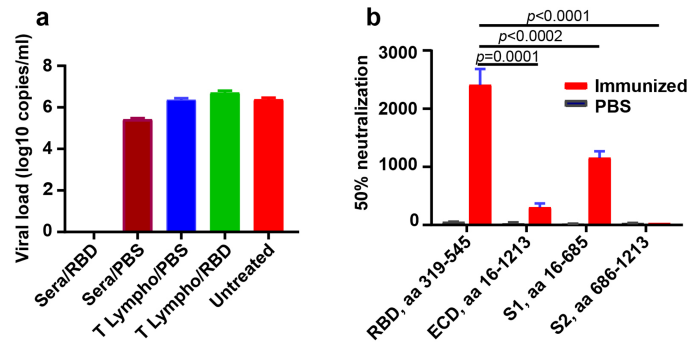


**Fig. 4 | The role of immune sera versus splenic T cells in the protective immunity in the vaccinated mice.** **a.** hACE2 mice with C57BL/6 background received 0.1 ml of the pooled sera or  $5 \times 10^7$  splenic T cells isolated from the mice with same C57BL/6 background 9 days after the third dose of the candidate vaccine or from the mice treated with PBS as a control. The mice were sacrificed 5 days after the challenge with live virus, and viral replication in lung tissues was evaluated. **b.** Infection of HEK293 cells expressing human ACE2 by SARS-CoV-2 pseudovirus was determined in the presence of mice sera at a series of 3-fold dilutions as described in Methods. The mice were immunized with 5  $\mu$ g recombinant RBD Protein (RBD, aa 319-545), the extracellular domain protein (ECD, aa 16-1213), S1-subunit protein (S1, aa 16-685) or S2-subunit protein (S2, aa, 686-1213) in the presence of aluminum hydroxide gel. 50% neutralization was presented as mean  $\pm$  SEM.



## Methods

### Bacterial strains and cell lines

All *E. coli* strains were cultured in Lysogeny broth (LB) medium (1% w/v Tryptone, 0.5% w/v yeast extract and 1% w/v NaCl) using a non-humidified shaker at 37 °C. *Spodoptera frugiperda* (Sf9) cells and *Trichoplusia ni* (Hi5) cells were individually maintained in the SIM SF medium and the SIMHF medium (Sino Biological, Beijing, China) using a non-humidified shaker at 27 °C. HEK293T and Huh-7 cells were maintained in Dulbecco's modified Eagle's medium (DMEM) supplemented with 10% fetal bovine serum (FBS), 100 units of Penicillin and 0.1 mg/ml of Streptomycin with 5% CO<sub>2</sub> at 37 °C.

### Gene cloning, protein expression and purification

The spike S protein RBD of SARS-CoV-2 for antigenicity evaluation was expressed using the Bac-to-Bac baculovirus expression system (Invitrogen). The coding sequence (codon optimized for insect cells) for the RBD region, which spans residues 319-545 of the spike of the SARS-CoV-2 Wuhan-Hu-1 isolate (accession number MN908947), were synthesized by Convenience Biology Corporation (Changzhou, Zhejiang Province, China). For gene cloning, a previously described gp67 signal peptide sequence<sup>7</sup> was first incorporated into the pFastBac1 vector via the BamH-I and EcoR-I restriction sites. The RBD gene was then sub-cloned into the modified vector via the EcoR-I and Hind-III sites. In addition, an 8×His tag was further added to the protein C terminus to facilitate protein purification. The sequencing-verified plasmid was subsequently transformed into *E. coli* DH10b cells to generate the recombinant bacmids.

For protein expression, the bacmid was first transfected into Sf9 insect cells using Lipoinsect Transfection Regent (Beyotime Biotechnology, Shanghai, China) according to the manufacturer's instructions. The cell culture supernatants, which contain the packaged recombinant baculoviruses, were harvested about 72 hours post transfection. The baculovirus was then passaged in Sf9 cells for 2-3 times before used for protein production in Sf9 cells.

For protein purification, the culture supernatants from the insect cells were collected about 72 hours after infection and passed through a 5-ml HisTrap excel column (GE Healthcare, Shanghai, China) for primary purification. The recovered proteins were further purified on a Superdex 200 Increase 10/300 GL column (GE Healthcare). Finally, the proteins were exchanged into a buffer consisting of 20 mM Tris-HCl (pH 8.0) and 150 mM NaCl for further use. Tag-free RBD protein was also prepared. The purity of the protein was determined by SDS-PAGE and visualized by staining with Coomassie blue and by western blotting using the rabbit anti-RBD antibody (Sino Biological).

Following the similar strategy described above, the SARS-CoV-2 ECD (extracellular domain, aa 16-1213), S1 (aa 16-685), and S2 (aa 686-1213) domain proteins were prepared using the Bac-to-Bac baculovirus expression system. In brief, the individual coding sequence was sub-cloned into the modified pFastBac1 vector, transposed into the bacmid in *E. coli* DH10b, and transfected into insect cells for recombinant baculovirus package and protein expression. The target proteins were then purified via affinity chromatography to a purity, as determined by SDS-PAGE and Coomassie blue staining, similar to that of the RBD protein.

### LC-MS/MS analysis to identify glycosylation sites

For MS test, the protein was first trypsin-digested as previously described<sup>23,24</sup>. In brief, the purified RBD protein was precipitated with 4 volumes of pre-cooled acetone at -20 °C overnight. The protein pellets were collected with centrifugation at 20,000 g for 10 min. After drying on ice, the protein pellets were dissolved in a denaturing buffer (5% 8 M urea in 50 mM NH<sub>4</sub>HCO<sub>3</sub>, v/v). The proteins were reduced with 20 mM DTT at 55 °C for 60 min, and alkylated with 55 mM iodoacetamide in the dark at room temperature for an additional 30 min. After

carbamidomethylation, the proteins were digested with trypsin (1:50 w/w) at 37 °C overnight.

After being desalted with C18 ZipTip (Millipore) according to the manufacturer's instructions, the digested peptides were analyzed by LC-MS/MS using an EASY-nano-LC 1200 coupled to a Q-Exactive HF-X (Thermo Scientific) without the trap column. Specifically, the peptide samples were loaded onto an in-house packed reversed-phase C18 analytical column (30 cm length×360 μm OD×75 μm ID, 3 μm particle, DIKMA) and were separated at a flow rate of 330 nL/min. The column oven temperature was 60 °C. Buffer A was 0.2% formic acid in water, and Buffer B was 80% ACN with 0.2% formic acid. A two hours gradient was applied with 3% B for 6 min, 3-48% B for 100 min, 48-100% B for 6 min, 100% B for 6 min, and 2% B for the last 2 min<sup>25</sup>. MS spectra were acquired with *m/z* 700-2000 and a resolution of 60,000 at *m/z* 200. The automatic gain control (AGC) was set at 2e5 with maximum fill time of 50 ms. For MS/MS scans, the Top 20 most intense parent ions were selected with a 2.0 *m/z* isolation window and fragmented using HCD with normalized collision energies of 20%/30%/30%<sup>26</sup>. The AGC value for MS/MS was set to a target value of 5e5, with a resolution of 3,000 and a maximum fill time of 250 ms. Parent ions with a charge state of *z* = 1, 8 or unassigned were excluded and the intensity threshold was 3.3e4. The dynamic exclusion period was 20 s. The temperature of the ion transfer capillary was set to 280 °C. The spray voltage was set to 2.8 kV.

For the identification of intact N-glycopeptides, all the raw files were searched with GPSeeker, developed by Tian's group<sup>9</sup>. In order to search matching precursor and fragment ions, the isotope peak abundance cutoff (IPACO), isotope peak mass-to-charge ratio (*m/z*) deviation (IPMD), and isotope peak abundance deviation (IPAD) were respectively set to 40%, 20 ppm and 50%. The search of intact N-glycopeptide spectrum matches (GPSMs) included the following parameters: Y1 ion, Top4; the minimum percentage of matched fragment ions of the peptide backbone, ≥10%; the minimum matched fragment ion of the N-glycan moiety, ≥1; TopN hits, N = 2 with Top1 hit(s) having the lowest P score; G-bracket, ≥1; and GF Score, ≥1. G-bracket for a given N-glycosite is defined as the number of peptide backbone b/y fragment ion pairs each of which can independently localize the N-glycosite. GF score for a given N-glycan sequence structure is defined as the number of structure-diagnostic fragment ions each of which can independently distinguish the structure from all the other putative structures with the same monosaccharide composition. After DB search of all the raw datasets, GPSMs were combined and intact N-glycopeptides with the lowest P score were chosen as the final IDs.

The MS Raw files were further searched against the RBD sequence with SEQUEST in Proteome Discoverer (version 2.3; Thermo Fisher Scientific). The precursor peptide mass tolerance was 10 ppm and the fragment ion mass tolerance was 0.02 Da. Two missing cleavages were allowed. Cysteine carbamidomethylation was set as a fixed modification. HexNAc (S/T), Hex(1)HexNAc(1)(S/T) and other potential O-glycosylation modifications with conventional oxidation of methionine and protein N-terminal acetylation were set as variable modifications<sup>9,23</sup>. Percolator was generated with false discovery rate (FDR) of 1%. All potential O-glycosylation sites were further manually confirmed by the b ions and y ions.

To determine the abundance of glycosylation, the number of MS/MS spectra of glycosylated peptides and their corresponding unmodified peptides were both counted. Glycosylation at different positions and glycosylation with different glycan isoforms on a peptide with identical sequence were combined.

### Surface plasmon resonance (SPR) analysis

Surface plasmon resonance (SPR)-based measurements were performed by Biacore 8K (GE Healthcare, Uppsala, Sweden), as described previously<sup>2</sup>. Human ACE2-Fc was captured to -100RU on Sensor Chip Protein A. For kinetic analysis, RBD protein was run across the chip in a 2-fold dilution series (1, 2, 4, 6, 8, 16, 32 nM), with another channel

# Article

set as control. Each sample bound across the antigen surface was dissociated by HBS-EP+ running buffer for 300 s at a flow rate of 30  $\mu$ L/min. Regeneration of the sensor chips was performed for 60 s using regeneration buffer (Glycine pH 1.5). The association and dissociation rate constants  $k_a$  and  $k_d$  were monitored respectively and the affinity value  $K_D$  was determined.

## Vaccine formulation and mice vaccinations

Alum-precipitated protein (alum protein) vaccines were prepared as described previously<sup>27</sup>. Briefly, the purified recombinant RBD protein at the different concentrations was added and incubated with mixing with aluminum hydroxide gel for one hour at 5 °C. The different formulations were prepared with the concentrations of 1-100  $\mu$ g/ml for protein and 1.21mg/ml for aluminum hydroxide gel.

BALB/c and C57BL/6 mice at 6 to 8 weeks of age were injected intramuscularly with different doses (0.1-20  $\mu$ g per mouse) of recombinant RBD and different intervals. For example, the mice were immunized with a single injection on Day 0 and collected sera on day 7, or with two vaccinations on day 0, day 7 and collected sera on day 21, compared with two doses on day 0, day 14 and collected sera on day 21. Also, we also investigated the third vaccine on day 21 or longer. Additional control animals were injected with aluminum hydroxide adjuvant [Al(OH)<sub>3</sub>], recombinant RBD or PBS alone. Pre-immune sera also were collected before starting the immunization and the sera were collected 7 days after each boost. Also, we also immunized the transgenic hACE2 mice with RBD vaccine and found that the mice had similar level of the antibodies against RBD protein, compared with the wild type mice (Extended Data Figure 4).

Sera were kept at 4 °C before use. Also, in an attempt to find the pathways through which our recombinant RBD may activate, recombinant RBD vaccine was injected into genetic deficient mice, *Cd4*<sup>-/-</sup>, *Cd8a*<sup>-/-</sup>, *Casp1*<sup>-/-</sup>, *Sting1*<sup>-/-</sup>, *Tlr2*<sup>-/-</sup>, *Tlr4*<sup>-/-</sup> (all from Jackson Laboratory), *Nlrp3*<sup>-/-</sup> (from Genentech), and *Il-1 $\beta$* <sup>-/-</sup> (Tokyo University of Science). All studies involving mice were approved by the Animal Care and Use Committee of Sichuan University.

## Identification of serum antibody against S protein RBD in patients and in mice using an ELISA assay

Blood samples were collected from the retro-orbital plexus of mice after each antigen boost. After coagulation at room temperature for 1-2 h, blood samples were spun in a centrifuge, 3000 rpm/min for 10 min at 4 °C. The upper serum layer was collected and stored at -20 °C. Recombinant RBD or S2 protein as a control was used to coat the flat-bottom 96-well plates (Thermo Scientific NUNC-MaxiSorp) at a final concentration of 1  $\mu$ g/ml in 50 mM carbonate coating buffer (pH 9.6) at 4 °C overnight. The following day, plates were washed 3 times with phosphate-buffered saline (PBS) containing 0.1% Tween 20 (PBST), and blocking solution containing 1% BSA in PBST was added, followed by 1 h incubation at room temperature. Serially diluted mouse sera were added and incubated at 37 °C for 1 h, and then washed the plates 3 times with PBST. Antibodies including goat anti-mouse IgG horseradish peroxidase (HRP)-conjugated antibody, or anti-mouse IgG1/IgM HRP-conjugated antibody were diluted 1/5000 in blocking solution and added to wells (100  $\mu$ l/well). After incubation for 1 h at room temperature, the plates were washed 5 times with PBST and developed with 3,3',5,5'-tetramethylbiphenyldiamine (TMB) for 10 min. The reactions were stopped with 50  $\mu$ l/well of 1.0 M H<sub>2</sub>SO<sub>4</sub> stop solution. The absorbance was measured on a microplate reader at 450 nm (A450). To measure the titer of RBD-specific antibodies induced by recombinant proteins, serum samples were serially diluted and measured by titration.

These studies were approved by the institutional ethics board of Sichuan Provincial People's Hospital. Data collection and analysis of cases were also required by the National Health Commission of the People's Republic of China to be part of a continuing public health

outbreak investigation. To investigate the potential immunogenicity of S protein RBD as vaccines in human, serum samples were collected from 16 patients infected with SARS-CoV-2 and 20 healthy donors detected with ELISA in similar way mentioned above. Briefly, the recombinant protein was used to coat 96-well microtiter plates, After blocking with 1% BSA, 1: 5 diluted sera were added and incubated, followed by four washes Bound Abs were detected with HRP-conjugated antibody (anti-human IgG/IgM antibody) at 1/2000 dilution. For the detection of IgM, serum samples were added to IgG sorbents and collect the supernatant for further detection centrifugation. All patients with COVID-19 were confirmed by RT-PCR using a 2019-nCoV nucleic acid detection kit. The use of this case series and healthy donors were approved by the institutional ethics board of Sichuan Provincial People's Hospital. Informed consent was obtained from all participants.

To investigate cell-mediated immune response, mice immunized with S protein RBD or PBS were sacrificed to isolate lymphocytes which were applied for IL-4, and IFN $\gamma$  ELISA assay. Briefly, the lymphocytes isolated from the spleens of the immunized mice or mice treated by PBS alone were cultured in RPMI medium 1640 supplied with 10% (vol/vol) FBS, 100 U/ml penicillin, 100  $\mu$ g/ml streptomycin, 1 mM pyruvate (all from Gibco), 50  $\mu$ M  $\beta$ -mercaptoethanol, and 20 U/ml IL-2 (all from Sigma-Aldrich). Simultaneously, 1  $\mu$ g/ml RBD protein was added to activate cells. These cells ( $1 \times 10^6$  per well) were incubated for 72 h at 37 °C. Cells cultured without RBD protein were used as negative control. The supernatants were collected for ELISA assay for the cytokines. Also, the potential memory lymphocytes against the recombinant RBD protein were identified by analyzing the phenotypes of these cultured lymphocytes by flow cytometry, as mentioned below in flow cytometry.

## Ethics approval

We obtained approval by the institutional ethics board of Sichuan Provincial People's Hospital. Data collection and analysis of cases were also required by the National Health Commission of the People's Republic of China to be part of a continuing public health outbreak investigation.

## Measurement of the inhibition of the RBD binding to cell surface ACE2

Binding assay of RBD-Fc with ACE2 was performed by flow cytometry as previously described<sup>28</sup>. Briefly, ACE2-positive Huh7 cells (a human hepatoma cell line) were collected and washed with Hanks' balanced salt solution. Recombinant SARS-CoV-2 RBD-Fc fusion protein was added to the cells to a final concentration of 0.1  $\mu$ g/ml in the presence or absence of the sera at a different dilution. The cells were incubated further at room temperature for 30 min. Cells were washed three times with HBSS and then stained with anti-human IgG-FITC conjugate (Sigma-Aldrich, St. Louis, MO, U.S.) at 1:50 dilution for an additional 30 min. After washing, the cells were fixed with 1% formaldehyde in PBS and processed by the NovoCyte Flow Cytometer (ACEA Biosciences, Inc.), and the results were analyzed with FlowJo V10 software.

## Neutralization of live SARS-CoV-2 infection and pseudovirus

To assess the neutralization of SARS-CoV-2 infection, Vero E6 cells ( $5 \times 10^4$ ) were seeded in 96-well plates and grown overnight. One hundred TCID<sub>50</sub> (50% tissue-culture infectious dose) of SARS-CoV-2 was preincubated with an equal volume of diluted sera before addition to cells. After incubation at 37 °C for 1 h, the mixture was added to Vero E6 cells. On day 3 after infection, the cytopathic effect (CPE) was recorded under microscope and the neutralizing titers of the dilutions of sera resulting in complete or EC 50 inhibition were calculated<sup>28</sup>.

A neutralization assay based on the pseudovirus was performed by measuring infection of ACE2-transfected 293T (293T/ACE2) cells as previously described<sup>13,16,29</sup>. Briefly, 293T cells were transfected with a plasmid encoding codon-optimized SARS-CoV 2 protein, a pLenti-EGFP vector and a gag/pol expression plasmid using polyetherimide (Sigma-Aldrich, 700193). Six hours post-transfection, the medium

was replaced with new complete culture medium. Forty-eight hours post-infection, the culture supernatants containing EGFP-expressing pseudoviruses were harvested, filtered through 0.45 µm pore-size (Millipore, SLHP033RB), concentrated with an ultrafiltration centrifugal tube and stored in 1 ml at aliquots at -80 °C until use. EGFP-expressing pseudotype viruses were produced by co-transfecting with a plasmid encoding codon-optimized SARS-CoV-2 S protein, a pLenti-EGFP vector and a gag/pol expression plasmid. Supernatants containing pseudovirus were harvest 48 h post-transfection and preincubated with the sera from the immunized mouse at various dilutions and control sera. After incubated for 1 hour at 37 °C, the mixture was added to ACE2-transfected 293T (293T/ACE2) cells to detect viral infectivity. Media was changed the following day and 48 h after infection, EGFP expression in infected cell was determined by fluorescent microscopy and flow cytometry.

Also, the some data on 50% neutralization activities is measured by SARS-CoV-2 pseudovirus that express spike protein, based on its backbone of VSV G pseudotype virus (G\*ΔG-VSV) were performed as described<sup>30</sup>. Briefly, with lipofectamine 3000 (Invitrogen, L3000015) reagents, the pcDNA3.1.S2 were transfected into 293T cells. Twenty-four hours after transfection, the 293T cells were infected with G\*ΔG-VSV with a multiplicity of four. After two hours, transfected cells were washed with PBS and replaced with fresh culture medium and incubated for 24 h. The culture supernatants containing pseudoviruses were harvested, filtered through 0.45 µm pore-size (Millipore, SLHP033RB) and stored at -80 °C until use. Infection of HEK293 cells expressing human ACE2 by SARS-CoV-2 pseudovirus was determined in the presence of mice, rabbit, or monkey sera at a series of 3-fold dilutions. In regard to SARS-CoV-2 pseudovirus that express spike protein, its backbone was provided by VSV G pseudotype virus (G\*ΔG-VSV) that packages expression cassettes for firefly luciferase instead of VSV-G in the VSV genome<sup>30</sup>.

### Challenge of the non-human primates (*Macaca mulatta*) with live SARS-CoV-2

All procedures involved in the non-human primates study were reviewed and approved by the Institutional Animal Care and Use Committee of Institute of Medical Biology, Chinese Academy of Medical Sciences, and performed in the ABSL-4 facility of Kunming National High-level Biosafety Primate Research Center, Yunnan, China. Twelve adult non-human primates (*Macaca mulatta*) (5-9 years old) were used for the challenge study with live SARS-CoV-2 and assigned into the following groups: (a) the group immunized with 40 µg RBD protein with Al(OH)<sub>3</sub> adjuvant per dose (n=4), (b) the group immunized with 20 µg with Al(OH)<sub>3</sub> per dose (n=3), (c) with PBS (control treatment, n=3), and (d) with Al(OH)<sub>3</sub> adjuvant alone (n=2). Non-human primates were immunized with two injections on day 0, day 7 via intramuscular route and then challenged with SARS-CoV-2 intranasally (0.5 ml, 10<sup>6</sup> pfu/ml) on day 28 after the first vaccination. A quantitative real-time reverse transcription-PCR (qRT-PCR) was employed to measure viral genomic RNA (gRNA), and viral subgenomic RNA (sgRNA, indicative of virus replication). Viral load in the lung tissues, throat swabs and anal swabs were measured by qRT-PCR. The primer and probe sequences used were derived from NP gene (Forward: 5'-GGGGAACCTCTCCTGCTAGAAT-3', Reverse: 5'-CAGACATTTGCTCTCAAGCTG-3', Probe: 5'-FAM-TTGCTGCTGCTTGACAGATT-TAMRA-3'), according to the sequences recommended by WHO and China CDC. SARS-CoV-2 E gene subgenomic mRNA (sgmRNA), indicative of virus replication, was assessed by RT-PCR using an approach similar to previously described<sup>31</sup>, based on The primer and probe sequences (Forward: 5'-GCTAGAGAACATCTAGACAAGAG-3', Reverse: 5'-ACACACGCATGACGACGTTATA-3', Probe: 5'-FAM-TGTGATCGGTAGGAATGACGCCAAGC-Quencher-3').

For paraffin-embedded sections, tissues were collected and fixed in 10% neutral buffered formalin, embedded in paraffin, and 5 µm sections were prepared for standard hematoxylin and eosin (H&E) staining.

### Adoptive therapy of splenic T cells or immune sera in the mice challenged with live SARS-CoV-2

All procedures involved in the animal study were reviewed and approved by the Institutional Animal Use and Care Committee of the Institute of Laboratory Animal Science, Peking Union Medical College. Mice studies were performed in an animal bio-safety level 3 (ABSL3) facility using HEPA-filtered isolators. The animal experiments of the infection of SARS-CoV-2 were performed by specific pathogen-free transgenic hACE2 mice established by the Institute of Laboratory Animal Science, Peking Union Medical College, China. Transgenic mice were generated by microinjecting a transgene carrying a mouse ACE2 promoter driving the human ACE2 coding sequence into the pronuclei of fertilized ova from ICR mice, as described in detail<sup>32</sup>. The transgenic hACE2 mice with C57BL/6 background<sup>33</sup> were provided by the National Institutes for Food and Drug Control (NIFDC, Beijing, China).

An adoptive therapy of splenic T cells was conducted previously<sup>23,34</sup>. hACE2 mice with C57BL/6 background received 5×10<sup>7</sup> splenic T cells isolated from either mouse with same C57BL/6 background 9 days after the third dose of the candidate vaccine or from the mice treated with PBS as a control. The adoptive therapy of the sera was described previously<sup>26</sup>. The adoptive therapy based on immune sera was performed using 0.1 ml of the pooled sera from the immunized mice at the same time. In addition, hACE2 mice with ICR background received 0.8 ml sera from the mice 7 days after a single dose of the vaccine and challenged with live SARS-CoV-2. The mice were sacrificed 5 days after the challenge with live virus, and viral loads in lung tissues, lung histopathological changes, and body weight change were evaluated. Viral load in the lung tissues were measured by qRT-PCR. Sections were stained by Hematoxylin and Eosin (H&E) and evaluated under light microscopy.

### Flow cytometry

T cells was evaluated with flow cytometry as previously described<sup>35</sup>. Mice immunized with S protein RBD or PBS were sacrificed to collect lymphocytes. The lymphocytes were cultured in RPMI medium 1640 supplied with 10% (vol/vol) FBS, 100 U/ml penicillin, 100 µg/ml streptomycin, 1 mM pyruvate (all from Gibco), 50 µM β-mercaptoethanol, 20 U/ml IL-2 (all from Sigma-Aldrich) for 72 h. At the same time, 1µg/ml S protein RBD was added to activate cells. Brefeldin A (BD Biosciences) was administrated 4-6 h before staining to block intracellular cytokine secretion. Cells were then washed in PBS (Gibco) and stained for 30 min at 4 °C with anti-CD8, anti-CD4, anti-CD44, anti-B220, anti-MHCII (all from BioLegend). Afterwards, cells were fixed and permeabilized to facilitate intracellular staining with anti-IFN $\gamma$ , and anti-IL-4 (all from BioLegend). Flow cytometry data were acquired on a NovoCyte Flow Cytometer (ACEA Biosciences, Inc.) and analyzed using FlowJo V10 software.

### Statistical analysis

Statistical analyses were performed using the Prism 8.0 (GraphPad Software). Comparisons among multiple groups across multiple time points were performed using a two-way ANOVA test with Tukey's multiple comparison post test. Comparisons among multiple groups were performed using a one-way ANOVA test followed by Tukey's multiple comparison post test. Comparisons between two groups were performed using an unpaired Student's t tests. P-values of < 0.05 were considered significant. \*P < 0.05, \*\*P < 0.01, \*\*\*P < 0.001, \*\*\*\*P < 0.0001. NS, no significance.

### Reporting summary

Further information on research design is available in the Nature Research Reporting Summary linked to this paper.

### Data availability

Reference SARS-CoV-2 RNA and protein sequences were downloaded from the NCBI database. All data are available in the main text or the supplementary materials.



23. Wang, Y. & Tian, Z. New Energy Setup Strategy for Intact N-Glycopeptides Characterization Using Higher-Energy Collisional Dissociation. *Journal of the American Society for Mass Spectrometry* **31**, 651-657 (2020).
24. Liu, M.-Q. et al. pGlyco 2.0 enables precision N-glycoproteomics with comprehensive quality control and one-step mass spectrometry for intact glycopeptide identification. *Nature communications* **8**, 1-14 (2017).
25. Yang, W., Ao, M., Hu, Y., Li, Q. K. & Zhang, H. Mapping the O-glycoproteome using site-specific extraction of O-linked glycopeptides (EXoO). *Molecular systems biology* **14** (2018).
26. Gupta, M., Mahanty, S., Bray, M., Ahmed, R. & Rollin, P. E. Passive transfer of antibodies protects immunocompetent and immunodeficient mice against lethal Ebola virus infection without complete inhibition of viral replication. *J Virol* **75**, 4649-4654 (2001).
27. Stadlmann, J. et al. Comparative glycoproteomics of stem cells identifies new players in ricin toxicity. *Nature* **549**, 538-542 (2017).
28. He, Y. et al. Receptor-binding domain of SARS-CoV spike protein induces highly potent neutralizing antibodies: implication for developing subunit vaccine. *Biochem. Biophys. Res. Commun.* **324**, 773-781 (2004).
29. He, Y., Lu, H., Siddiqui, P., Zhou, Y. & Jiang, S. Receptor-binding domain of severe acute respiratory syndrome coronavirus spike protein contains multiple conformation-dependent epitopes that induce highly potent neutralizing antibodies. *J Immunol* **174**, 4908-4915 (2005).
30. Nie, J. et al. Establishment and validation of a pseudovirus neutralization assay for SARS-CoV-2. *Emerging microbes & infections* **9**, 680-686 (2020).
31. Wölfel, R. et al. Virological assessment of hospitalized patients with COVID-2019. *Nature* **581**, 465-469 (2020).
32. Bao, L. et al. The pathogenicity of SARS-CoV-2 in hACE2 transgenic mice. *Nature* (2020).
33. Sun, S. H. et al. A Mouse Model of SARS-CoV-2 Infection and Pathogenesis. *Cell Host Microbe* (2020).
34. Zhao, J., Zhao, J. & Perlman, S. T cell responses are required for protection from clinical disease and for virus clearance in severe acute respiratory syndrome coronavirus-infected mice. *J Virol* **84**, 9318-9325 (2010).
35. Xiao, Y. et al. Adsorption of recombinant poxvirus L1-protein to aluminum hydroxide/CpG vaccine adjuvants enhances immune responses and protection of mice from vaccinia virus challenge. *Vaccine* **31**, 319-326 (2013).

**Acknowledgements** We thank Mr. Zhen Li, Mr. Guo Wei, Mr. Qian Chen, Miss. Hong Yan, Mr. Xincheng Zhou, Miss. Xiaofeng Wu, Mr. Feiyu Fu, Mr. Haotian Yang and Miss. Xia Wu for their assistance in maintaining mice facility, the collection of sera, cell culture, ELISA assay and other technical support. This work was supported by the National Key Research and

Development Program of China (No. 2016YFA0201402), National Natural Science Foundation Regional Innovation and Development (U19A2003), the National Major Scientific and Technological Special Project for "Significant New Drugs Development" (No. 2018ZX09733001), the projects for the vaccine by the Ministry of Science and Technology, National Health Commission, Ministry of education of the People's Republic of China, Sichuan province, National Key Research and Development Project of China (Grant No. 2016YFD0500304). The special research fund on COVID-19 of Sichuan Province (grant No. 2020YFS0010) and the special research fund on COVID-19 of West China Hospital Sichuan University (grant No. HX-2019-nCoV-004). Macao Science and Technology Development Fund (FDCT).

**Author contributions** X.W.W., G.W.L., K.Z., Y.Q.W. conceived and supervised the research, and designed the experiments. Z.M.C., F.L.Y., F.Y., S.L., H.C., Y.Z., L.Y., J.L., Y.H. and D.L. performed gene cloning, expression and protein purification, Y.Q.G., H.X.D., Z.L.W., J.L.Y., Z.X.T., L.Z.D. W.C. and Y.P. performed LC-MS/MS analysis to identify glycosylation sites, C.Q., L.L.B., H.G., W.D., Y.F.X., Q.L., F.D.L., S.Y.W., G.P.W., P.Y. and Y.J.Q. performed the challenge of the mice with live SARS-CoV-2, A.P.T., W.J.H., Y.C.W. and Y.H.L. performed neutralization of pseudovirus infection and measurement of inhibition of the S protein RBD binding to cell-expressed ACE2. J.Y.Y., X.W.W., Z.F.B., F.M., M.L., G.B.S., Z.W.Z., X.B.C. C.F.F. and Z.Y.Q. performed vaccine formulation and mice vaccinations. X.B.C., X.Z.P., S.Y.L., H.Q.L., Y.Y., Y.Z., W.H.Y., M.L.Y., J.W.X., J.B.W., H.Y.L., H.X.W., D.X.K., Z.T.H., W.G., Y.L.H., X.R.S., C.C.Z., H.X., S.H.Y., L.C. performed vaccine formulation and vaccinations in rabbits and monkeys. X.W.W., J.Y.Y., Z.F.B., F.M., M.L., S.Y.C., G.B.S., Z.L.Y., F.S.W., M.S. performed identification of serum antibody against S protein RBD, J.L.Y. and X.H.J. performed surface plasmon resonance (SPR) analysis, H.L., X.L. and Z.Q.Z. performed flow cytometry. X.W.W., J.Y.Y., W.W., M.N.W. and W.Q.H. S.G., C.H.H., J.W.L. P.P.L. J.Y.-N.L. X.L.M. K.Z. analyzed and interpreted the data. J.Y.-N.L. and K.Z. assisted the adjustments of directions and interpretation of the mechanistic aspects of the results. X.W.W., J.Y.-N.L., K.Z., G.W.L., and M.W. contributed to writing the manuscript.

**Competing interests** G.L., J.L., J.Y.N., L., G. S., L. Y., W. Y., J.L. Y., X. W., Z. W., W.W., Y.W., K.Z., Z. Z. filed patents on vaccine technologies.

#### Additional information

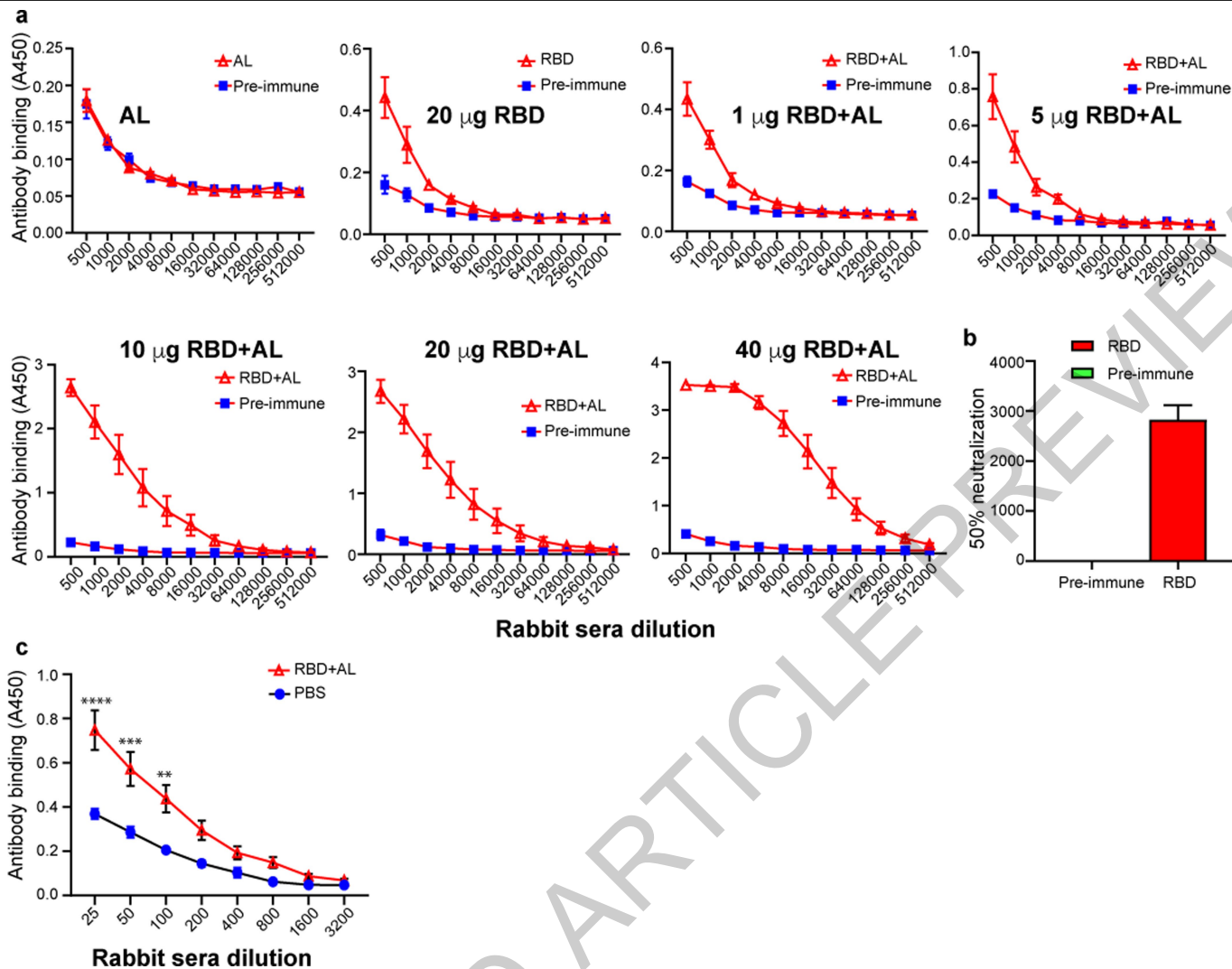
**Supplementary information** is available for this paper at <https://doi.org/10.1038/s41586-020-2599-8>.

**Correspondence and requests for materials** should be addressed to K.Z., G.L., X.W., K.Z., G.L. or X.W.

**Peer review information** *Nature* thanks Wolfgang Baumgärtner and the other, anonymous, reviewer(s) for their contribution to the peer review of this work.

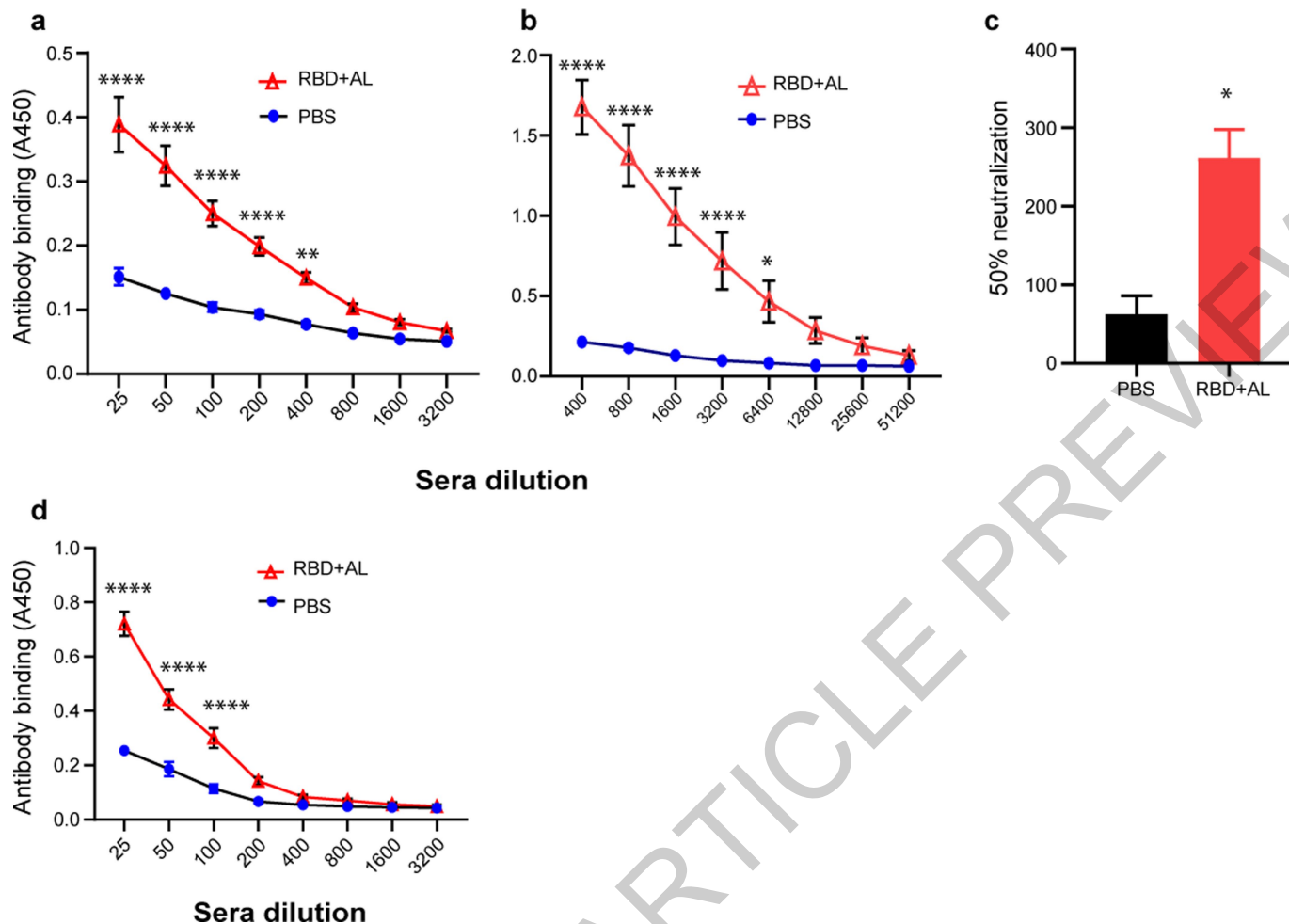
**Reprints and permissions information** is available at <http://www.nature.com/reprints>.

ACCELERATED ARTICLES



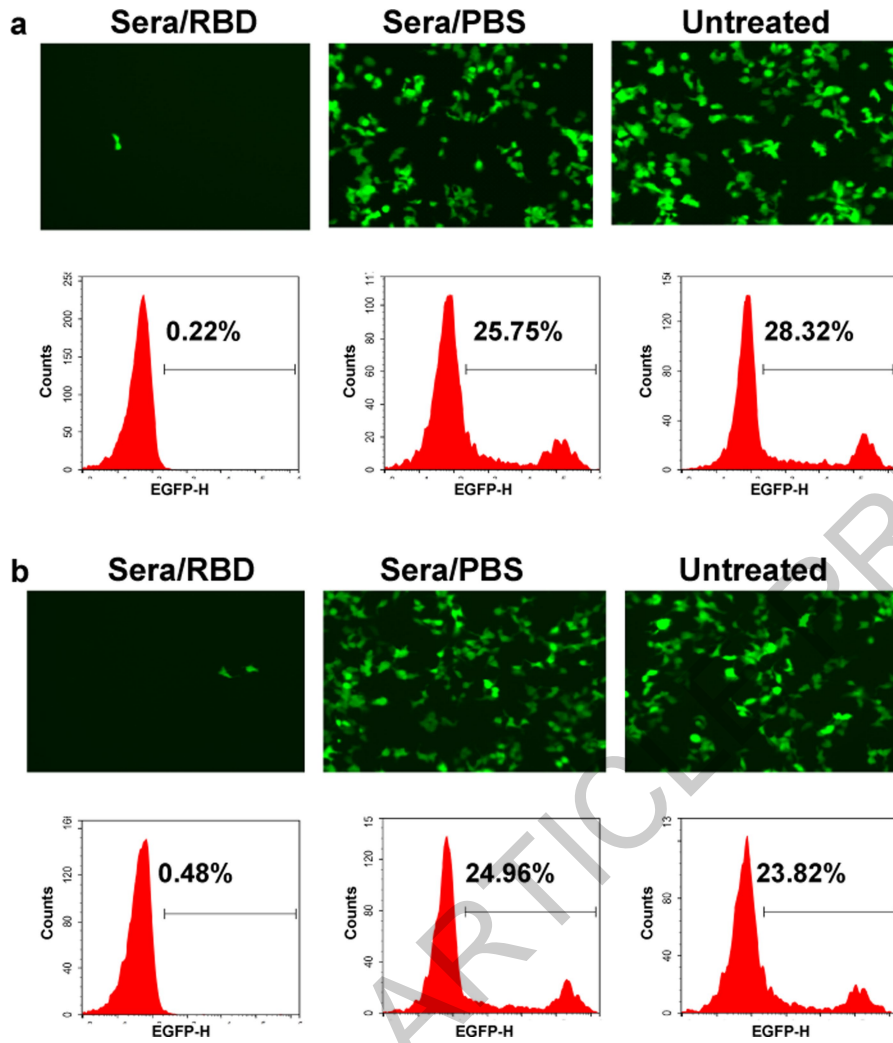
**Extended Data Fig. 1 | Identification of serum antibody against S protein RBD and neutralizing antibody against SARS-CoV-2 pseudovirus in rabbits.** **a.** The rabbits were immunized with 1-40  $\mu$ g recombinant RBD protein per rabbit in 500  $\mu$ l in the presence of aluminum hydroxide [Al(OH)<sub>3</sub>], or Al(OH)<sub>3</sub> or PBS alone. Rabbits were immunized with three vaccinations on day 0, day 14 and day 21, collected sera 7 days after each boost. Sera were collected from the rabbits 7 days after the third vaccination and were tested at different dilution for IgG against S protein RBD using ELISA. Data are presented as the mean  $\pm$  SEM of six rabbits' sera in each group, except for four rabbits in the AL group. AL: Al(OH)<sub>3</sub>, RBD: recombinant RBD protein, RBD+AL: the addition of the recombinant RBD protein to Al(OH)<sub>3</sub>. **b.** Potent neutralization of SARS-CoV-2 pseudovirus infection by the sera from the rabbit immunized with

recombinant RBD vaccine. Infection of HEK293 cells expressing human ACE2 by SARS-CoV-2 pseudovirus was determined in the presence of rabbit sera at a series of 3-fold dilutions. Percentage of neutralization was presented as mean  $\pm$  SEM. The sera from the rabbits immunized 7 days after the third vaccination with the dose of 20  $\mu$ g recombinant RBD protein per rabbit in 500  $\mu$ l in the presence of aluminum hydroxide in the same as a. The neutralization assay of SARS-CoV-2 pseudovirus was performed as described in Methods. **c.** The rabbits were immunized in the same way as a, Sera were collected from the rabbits 7 days after the first vaccination with the dose of 40  $\mu$ g recombinant RBD protein and were tested at different dilution for IgM against S protein RBD using ELISA.



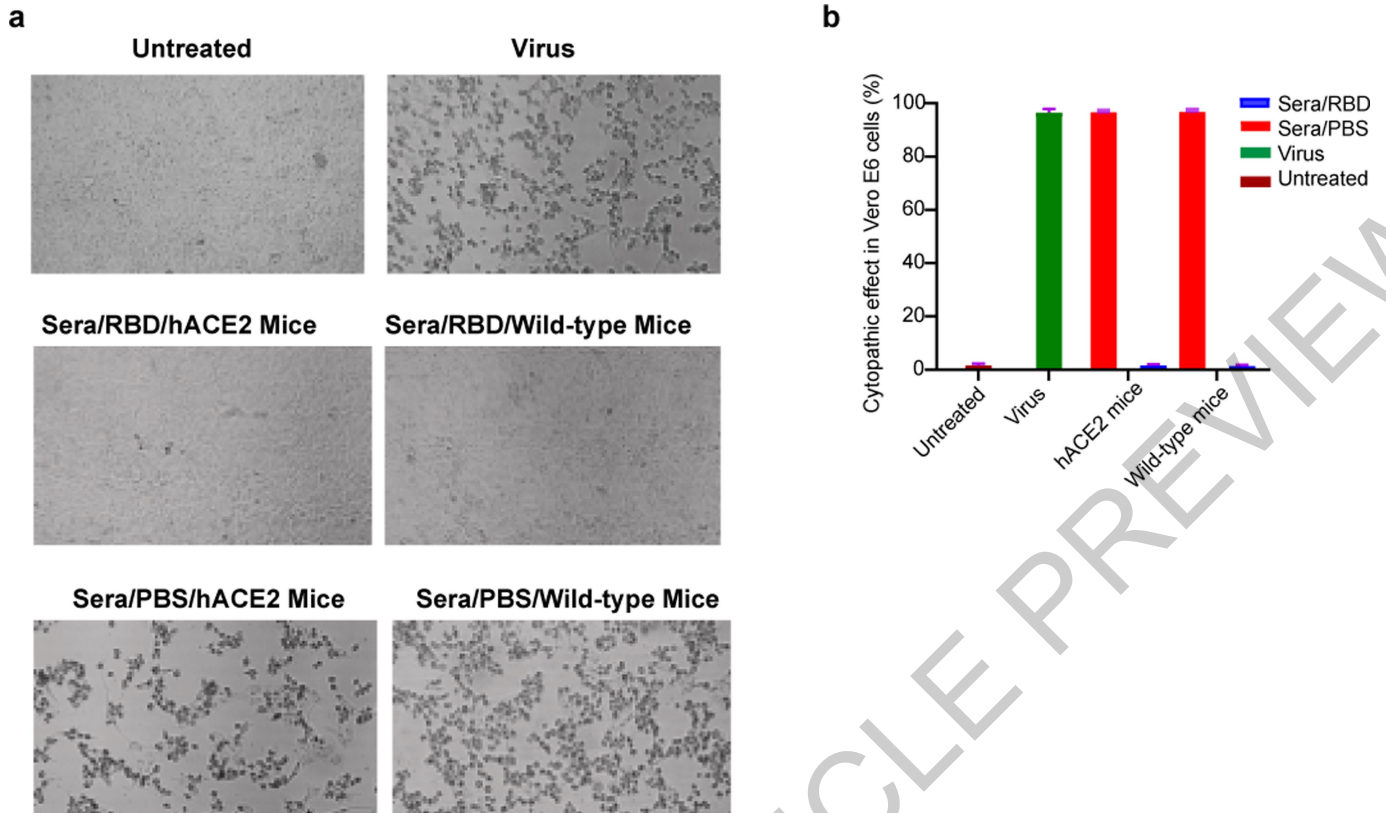
**Extended Data Fig. 2 | Identification of serum antibody against S protein RBD and in non-human primates.** The non-human primates (*Macaca mulatta*) were immunized with 40  $\mu$ g recombinant RBD protein per monkey in 1 ml in the presence of aluminum hydroxide on day 0 and day 7, and sera were obtained at 7 day (a) and 14 days (b) after the first vaccination or before the vaccination (Pre-immune). Also, the monkeys were treated with PBS as a control. Sera were tested at the different dilution for IgG against recombinant RBD protein using ELISA as described in Methods. Data are presented as the mean  $\pm$  SEM of 10 monkey sera in each group. P-values were determined by two-way ANOVA.

P-values indicated RBD+AL vs PBS groups in IgG level. (c) The neutralization of the infection of SARS-CoV-2 pseudovirus by the sera from the non-human primates. The neutralization assays were performed with the sera from monkeys 14 days after the first vaccination as in b. 50% neutralization (EC50) was presented as mean  $\pm$  SEM. The neutralization assay of SARS-CoV-2 pseudovirus was described in Methods. **d**. The rabbits were immunized in the same way as a, Sera were collected from the rabbits 7 days after the first vaccination with the dose of 40  $\mu$ g recombinant RBD protein and were tested at different dilution for IgM against S protein RBD using ELISA.



**Extended Data Fig. 3 | The neutralization of the infection of SARS-CoV-2 pseudovirus by the sera from mice or rabbits.** a. Supernatants containing SARS-CoV-2 pseudovirus were preincubated with the sera from mice which was serially diluted 2-fold. After incubated for 1 hour at 37 °C, the mixture was added to ACE2-transfected 293T (293T/ACE2) cells to detect viral infectivity. The number of green fluorescent protein (GFP) expression in the infected cell was determined by fluorescent microscopy and flow cytometry. Sera/RBD

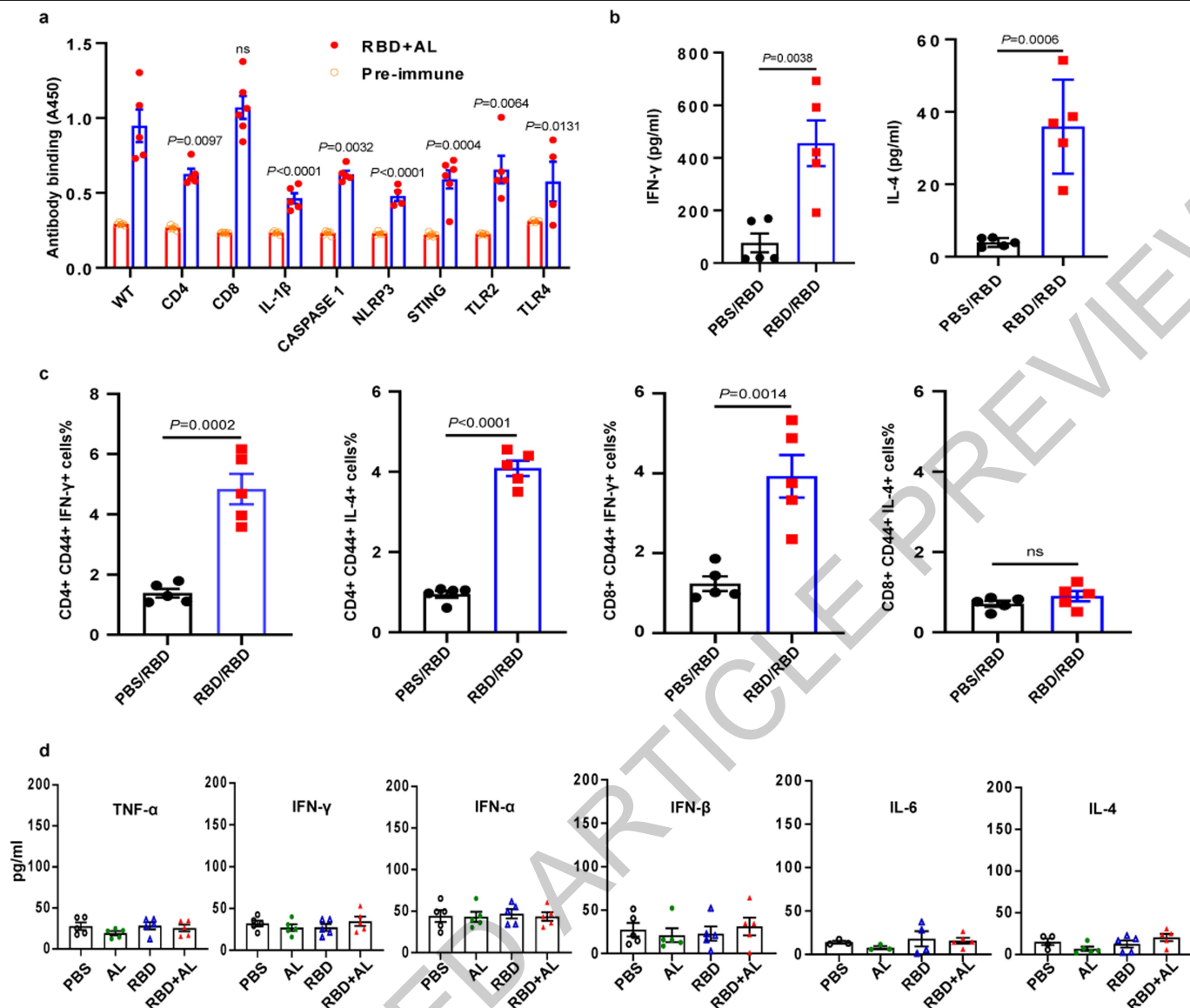
(sera pooled from 5 mice immunized with RBD vaccine day 14 after the first vaccination) and Sera/PBS (sera from the mice treated by PBS as a control), Untreated (infection with SARS-CoV-2 pseudovirus without sera). b. The neutralization of the infection of SARS-CoV-2 pseudovirus was performed using the sera from rabbits 14 days after the first vaccination in the same way as a.



**Extended Data Fig. 4 | The induction of the neutralizing antibodies against live SARS-COV-2 in the transgenic hACE2 mice and the wild-type mice.**

**a.** The transgenic hACE2 mice and the wild-type mice were immunized with 10  $\mu$ g recombinant RBD protein per mouse in 50  $\mu$ l in the presence of aluminum hydroxide, compared with the treatment with PBS alone. Sera were collected from the mice 14 days after the second vaccination. To assess the neutralization of SARS-COV-2 infection, Vero E6 cells ( $5 \times 10^4$ ) were pre-load in 96-well plates and grown overnight. One hundred TCID<sub>50</sub> (50% tissue-culture infectious

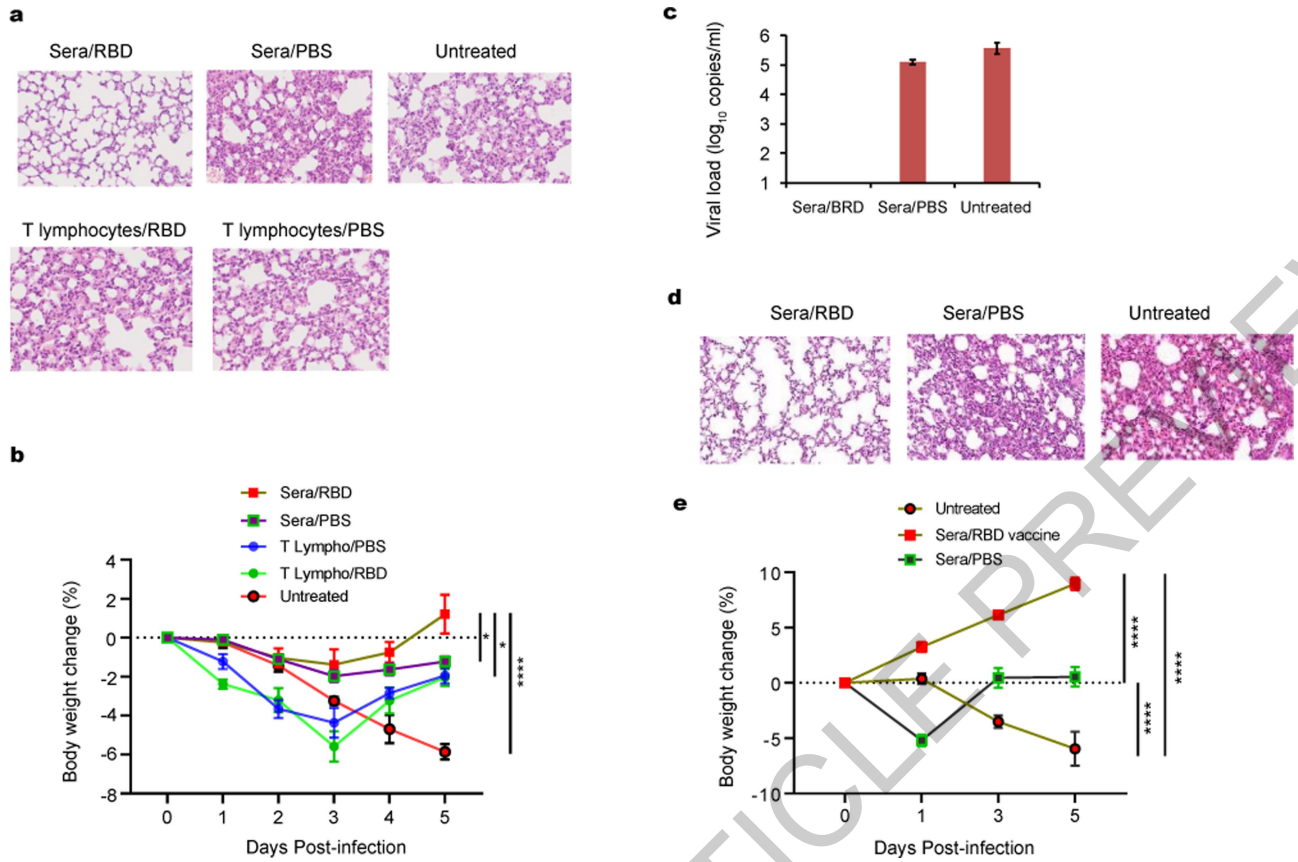
dose) of SARS-CoV-2 was preincubated with an equal volume of diluted sera before addition to cells. After incubation at 37 °C for 1 h, the mixture was added to Vero E6 cells. The cytopathic effect (CPE) was recorded under microscope and the neutralizing titers of the dilutions of sera resulting in complete inhibition were calculated. **b.** The percentage of the number of the cells with cytopathic effect was calculated under microscope and presented as mean  $\pm$  SD.



**Extended Data Fig. 5 | The pathways involved with the recombinant RBD stimulation and cellular immune response.** **a.** Wild-type C57BL/6 mice and mice deficient in *Cd4<sup>-/-</sup>*, *Cd8 $\alpha$ <sup>-/-</sup>*, *Tlr2<sup>-/-</sup>*, *Tlr4<sup>-/-</sup>*, *Sting1<sup>-/-</sup>*, *Casp1<sup>-/-</sup>*, *Nlrp3<sup>-/-</sup>*, and *Il-1 $\beta$ <sup>-/-</sup>* were immunized with the recombinant RBD protein (5  $\mu$ g per mouse) and sera were collected on day 7 after the first dose of vaccine and were tested for the antibody against RBD at the dilution of 1:25. The data are expressed as mean $\pm$ SEM. *P*-values were determined by two-way ANOVA (4-6 mice per group). Similar results were repeated in two independent experiments. **b.** Cytokines produced by the spleen lymphocytes were detected by ELISA under the stimulation of the recombinant RBD. Mice immunized with the candidate RBD vaccine or treated with PBS were sacrificed 7 days after the first dose of vaccine to isolate lymphocytes which were then stimulated with recombinant RBD for three days, and the supernatants were

collected for the level of secreted IL-4 and IFN- $\gamma$  by ELISA assays, as described in Methods. The data are expressed as mean $\pm$ SD. *P*-values were determined by unpaired Student's *t* tests (5 mice per group). Similar results were repeated in three independent experiments. **c.** The lymphocytes in the spleen were collected from the mice with the recombinant RBD (5  $\mu$ g per mouse) 7 days after the first vaccination and were incubated with RBD for three days, and then RBD-reactive memory CD4 or CD8 was analyzed by flow cytometry by gating CD4+ or CD8+ CD44<sup>high</sup> + B220- MHCII- IFN- $\gamma$ + or IL-4+, as described in Method. Similar results were repeated in three independent experiments. **d.** Sera were collected from the mice 7 days after the first dose of vaccine and plasma level of cytokines such as TNF- $\alpha$ , IFN- $\gamma$ , IFN- $\alpha$ , IFN- $\beta$ , IL-6, IL-4 were measured by ELISA. AL: Al(OH)<sub>3</sub>, RBD: recombinant RBD, RBD+AL: the addition of the recombinant RBD to Al(OH)<sub>3</sub>.





**Extended Data Fig. 6 | Adoptive therapy of immune sera from the vaccinated mice.** **a.** hACE2 mice with C57BL/6 background received 0.1 ml of the pooled sera or  $5 \times 10^7$  splenic T cells isolated from the mice with same C57BL/6 background 9 days after the third dose of the candidate vaccine or from the mice treated with PBS as a control. The mice were sacrificed 5 days after the challenge with live virus, and viral replication in lung tissues (Figure 4a), lung histopathological changes (a), and body weight change (b) were evaluated. viral replication in lung tissues was evaluated. hACE2 mice with

ICR background received 0.8 ml sera from the mice 7 days after a single dose of the vaccine and challenged with live SARS-CoV-2. The mice were sacrificed 5 days after the challenge with live virus, and viral replication in lung tissues (c), lung histopathological changes (d), and body weight change (e) were evaluated. Adoptive therapy was described in Methods. Sera/RBD (sera pooled from the mice immunized with RBD vaccine) and Sera/PBS (sera from the mice treated by PBS as a control), Untreated (infection with live SARS-CoV-2 without sera).

## Reporting Summary

Nature Research wishes to improve the reproducibility of the work that we publish. This form provides structure for consistency and transparency in reporting. For further information on Nature Research policies, see [Authors & Referees](#) and the [Editorial Policy Checklist](#).

### Statistics

For all statistical analyses, confirm that the following items are present in the figure legend, table legend, main text, or Methods section.

n/a Confirmed

- The exact sample size ( $n$ ) for each experimental group/condition, given as a discrete number and unit of measurement
- A statement on whether measurements were taken from distinct samples or whether the same sample was measured repeatedly
- The statistical test(s) used AND whether they are one- or two-sided  
*Only common tests should be described solely by name; describe more complex techniques in the Methods section.*
- A description of all covariates tested
- A description of any assumptions or corrections, such as tests of normality and adjustment for multiple comparisons
- A full description of the statistical parameters including central tendency (e.g. means) or other basic estimates (e.g. regression coefficient) AND variation (e.g. standard deviation) or associated estimates of uncertainty (e.g. confidence intervals)
- For null hypothesis testing, the test statistic (e.g.  $F$ ,  $t$ ,  $r$ ) with confidence intervals, effect sizes, degrees of freedom and  $P$  value noted  
*Give  $P$  values as exact values whenever suitable.*
- For Bayesian analysis, information on the choice of priors and Markov chain Monte Carlo settings
- For hierarchical and complex designs, identification of the appropriate level for tests and full reporting of outcomes
- Estimates of effect sizes (e.g. Cohen's  $d$ , Pearson's  $r$ ), indicating how they were calculated

*Our web collection on [statistics for biologists](#) contains articles on many of the points above.*

### Software and code

Policy information about [availability of computer code](#)

Data collection

1. Affinity and kinetics data for RBD were collected using Biacore 8K by GE Healthcare (General Electric Company).
2. Flow cytometric data were collected using LSRFortessa (BD Biosciences) or NovoCyte (ACEA bioscience. Inc).
3. Pathologic slides were digitized using Olympus IX73 microscope (Olympus Corporation) using 20x/0.8NA objective and filters for A488.
4. Western blot data were collected using Clinx ChemiScope Series (Clinx Science Instrument Co., Ltd).
5. Enzyme linked Immunosorbent Assay data were collected using CYTATION 3 Imaging Reader (BioTek Instruments, Inc. ).

Data analysis

CellSens Standard software  
NovoExpress 1.4.1  
GraphPad Prism version 8.0,  
Photoshop(Adobe),  
Biacore Insight Evaluation Software,  
Gen5 version 3.05,  
PyMOL 1.3

For manuscripts utilizing custom algorithms or software that are central to the research but not yet described in published literature, software must be made available to editors/reviewers. We strongly encourage code deposition in a community repository (e.g. GitHub). See the Nature Research [guidelines for submitting code & software](#) for further information.



## Data

Policy information about [availability of data](#)

All manuscripts must include a [data availability statement](#). This statement should provide the following information, where applicable:

- Accession codes, unique identifiers, or web links for publicly available datasets
- A list of figures that have associated raw data
- A description of any restrictions on data availability

All reasonable requests will be considered and granted by a data access committee consisted of YQ W, KZ, XW W

## Field-specific reporting

Please select the one below that is the best fit for your research. If you are not sure, read the appropriate sections before making your selection.

- Life sciences  Behavioural & social sciences  Ecological, evolutionary & environmental sciences

For a reference copy of the document with all sections, see [nature.com/documents/nr-reporting-summary-flat.pdf](https://www.nature.com/documents/nr-reporting-summary-flat.pdf)

## Life sciences study design

All studies must disclose on these points even when the disclosure is negative.

Sample size	Sample sizes were determined based on our and other investigators experience. No statistical methods were used to predetermine sample size.
Data exclusions	No data were excluded from the analysis.
Replication	Most of Experiments were repeated with at least two biologically independent for all results presented in the manuscript.
Randomization	Mice of 6- to 10-week old were matched by age and sex and randomly assigned to different treatment groups.
Blinding	Researchers were not blinded in the process of experiments or data analysis since all of the findings are supported by quantitative measurement.

## Reporting for specific materials, systems and methods

We require information from authors about some types of materials, experimental systems and methods used in many studies. Here, indicate whether each material, system or method listed is relevant to your study. If you are not sure if a list item applies to your research, read the appropriate section before selecting a response.

### Materials & experimental systems

n/a	Involvement in the study
<input type="checkbox"/>	<input checked="" type="checkbox"/> Antibodies
<input type="checkbox"/>	<input checked="" type="checkbox"/> Eukaryotic cell lines
<input checked="" type="checkbox"/>	<input type="checkbox"/> Palaeontology
<input type="checkbox"/>	<input checked="" type="checkbox"/> Animals and other organisms
<input type="checkbox"/>	<input checked="" type="checkbox"/> Human research participants
<input checked="" type="checkbox"/>	<input type="checkbox"/> Clinical data

### Methods

n/a	Involvement in the study
<input checked="" type="checkbox"/>	<input type="checkbox"/> ChIP-seq
<input type="checkbox"/>	<input checked="" type="checkbox"/> Flow cytometry
<input checked="" type="checkbox"/>	<input type="checkbox"/> MRI-based neuroimaging

## Antibodies

### Antibodies used

anti-CD8-FITC, Applicable: FCM, Provide supplier name: BioLegend, Cat: 100706, Clone: 53-6.7, Lot: B278606  
 anti-CD4-APC, Applicable: FCM, Provide supplier name: BioLegend, Cat: 100412, Clone: GK1.5, Lot: B293107  
 anti-MHC-II-PE-Cy7, Applicable: FCM, Provide supplier name: BioLegend, Cat: 107630, Clone: M5/114.15.2, Lot: B199459  
 anti-CD45R-PerCP/Cy5.5, Applicable: FCM, Provide supplier name: BioLegend, Cat: 103236, Clone: RA3-6B2, Lot: B295257  
 anti-CD44-BV510, Applicable: FCM, Provide supplier name: BioLegend, Cat: 103044, Clone: IM7, Lot: B298812  
 anti-IFN- $\gamma$ -PE, Applicable: FCM, Provide supplier name: BD Bioscience, Cat: 554412, Clone: XMG1.2, Lot: 3217951  
 anti-IL-4-BV421, Applicable: FCM, Provide supplier name: BioLegend, Cat: 504120, Clone: 11B11, Lot: B282852  
 rabbit anti-ACE2, Applicable: FCM, Provide supplier name: Sino Biological, Cat: 10108-RP01, Clone: Polyclonal Rabbit IgG, Lot: GR3331742-1  
 Donkey anti-rabbit IgG-FITC, Applicable: FCM, Provide supplier name: BioLegend, Cat: 406403, Clone: Poly4064, Lot: B228075  
 anti-His Tag-PE, Applicable: FCM, Provide supplier name: BioLegend, Cat: 362603, Clone: J095G46, Lot: B269138  
 Mouse IgG-HRP, Applicable: ELISA, Provide supplier name: southern biotech, Cat: 0107-05

Mouse IgM-HRP, Applicable: ELISA, Provide supplier name: southern biotech, Cat: 1021-05, Lot: I2015-YF97C.

#### Validation

Antibodies were chosen based on the available literature. Quality of the antibodies used in the study was tested by manufacturer or relevant references cited on the manufacturer's website. Additional information on validation can be found on the manufacturers' websites.

## Eukaryotic cell lines

Policy information about [cell lines](#)

#### Cell line source(s)

HUH-7 cells (JCRB JCRB0403), HEK293T cells (ATCC CRL-11268)

#### Authentication

Cell lines were authenticated by morphology

#### Mycoplasma contamination

Neither of the cell lines used in this study tested positive for Mycoplasma.

#### Commonly misidentified lines (See [ICLAC](#) register)

No commonly misidentified lines were used in this study.

## Animals and other organisms

Policy information about [studies involving animals](#); [ARRIVE guidelines](#) recommended for reporting animal research

#### Laboratory animals

Purchased from Jackson Laboratory  
B6N.129S2-Casp1tm1Flv/J, (Jax #016621)  
B6.129S6-Cd4tm1Knw/J, (Jax #002269)  
B6.129S2-Cd8atm1Mak/J, (Jax #002665)  
C57BL/6J-Sting1gt/J, (Jax #17537)  
B6.129-Tlr2tm1Kir/J, (Jax #004650)  
B6.B10ScN-Tlr4lps-del/JthJ, (Jax #007227)  
B6(Cg)-Ifnar1tm1.2Ees/J, (Jax #028288)

Purchased from Genentech, Inc., USA  
Asc-/-  
Nlrp3-/-

Provided by Tokyo University of Science  
Il-1 $\beta$ -/-

Purchased from Beijing Vital River Laboratory Animal Technology  
CD-1<sup>®</sup>(ICR) IGS  
NIH(S)  
C57BL/6N  
Transgenic hACE2 mice with ICR background were provided by the Institute of Laboratory Animal Science, Peking Union Medical College, China.  
Transgenic hACE2 mice with C57BL/6 background<sup>35</sup> were provided by the National Institutes for Food and Drug Control (NIFDC, Beijing, China)  
Rabbits Purchased from Shangdong Benming Biotechnology Limited Company, China, Production License No : SCXX(Lu)2017-0003.  
Mon-human primates (Macaca mulatta) for the immunization and challenge provided by National Kunming High-level Biosafety Primate Research Center, Institute of Medical Biology, Chinese Academy of Medical Sciences and Peking Union Medical College, Yunnan China.  
Mon-human primates (Macaca mulatta) for the safety study Purchased from Sichuan Hensu Biotechnology Limited Company, Production License No: SCXX (Chuan) 2019-029.

#### Wild animals

No wild animals were used in this study.

#### Field-collected samples

No field-collected samples were used in the study.

#### Ethics oversight

All animal studies carried out were approved by the Animal Care and Use Committee of Sichuan University (Chengdu, Sichuan, China).  
Transgenic hACE2 mice were approved by the Animal Care and Use Committee, the Institute of Laboratory Animal Science, Peking Union Medical College, China.  
All procedures involved in the immunization and challenge in the non-human primates study were reviewed and approved by the Institutional Animal Care and Use Committee of Institute of Medical Biology, Chinese Academy of Medical Science, and performed in the ABSL-4 facility of Kunming National High-level Biosafety Primate Research Center, Yunnan, China.  
All procedures involved in the immunization in rabbits and safety study in the non-human primates were reviewed and approved by the Institutional Animal Care and Use Committee, National Chengdu Center for Safety Evaluation of Drugs, Chengdu, China.

Note that full information on the approval of the study protocol must also be provided in the manuscript.

## Human research participants

Policy information about [studies involving human research participants](#)

### Population characteristics

In order to investigate the potential immunogenicity of S protein RBD as vaccines in human, serum samples were collected from 16 patients infected with SARS-CoV-2 and 20 healthy donors detected with ELISA. All 16 patients with COVID-19 were confirmed by RT-PCR using a 2019-nCoV nucleic acid detection kit. In addition, 20 healthy donors for blood as a control. 16 patients including 12 female, 4 male, age from 23 to 76 years old, common symptoms at onset of illness were fever, fatigue, dry cough, myalgia. Chest computed tomographic images show ground glass opacity to varying degree.

### Recruitment

This study is not a clinical trial. The blood from 16 patients and 20 healthy donors only for confirming the existence of the antibody reactive to RBD protein of SARS-CoV-2.

### Ethics oversight

This case series and healthy donors were approved by the institutional ethics board of Sichuan Provincial People's Hospital

Note that full information on the approval of the study protocol must also be provided in the manuscript.

## Flow Cytometry

### Plots

Confirm that:

- The axis labels state the marker and fluorochrome used (e.g. CD4-FITC).
- The axis scales are clearly visible. Include numbers along axes only for bottom left plot of group (a 'group' is an analysis of identical markers).
- All plots are contour plots with outliers or pseudocolor plots.
- A numerical value for number of cells or percentage (with statistics) is provided.

### Methodology

#### Sample preparation

##### Splenocytes activation

T cells activation was evaluated with flow cytometry. Mice immunized with S1-RBD or PBS were sacrificed to collect splenocytes. After lysis of red blood cells, splenocytes were cultured in RPMI medium 1640 supplied with 10% (vol/vol) FBS, 100 U/ml penicillin, 100 µg/ml streptomycin, 1 mM pyruvate (all from Gibco), 50 µM β-mercaptoethanol (Amresco), and 20 U/ml IL-2 (Sigma-Aldrich) for 72 h. At the same time, 10 µg/ml S1-RBD was added to activate cells. Brefeldin A (BD Biosciences) was administered 4-6h before staining to block intracellular cytokine secretion. Cells were then washed in PBS (Biosharp) and stained for 30 min at 4 °C with anti-CD8a-FITC (53-6.7), anti-CD4-APC (GK1.5), anti-MHC-II-PE-Cy7 (M5/114.15.2), anti-CD45R-PerCP/Cy5.5 (RA3-6B2) and anti-CD44-BV510 (IM7) (all from BioLegend). Afterwards, cells were fixed and permeabilized to facilitate intracellular staining with anti-IFNγ-PE (XMG1.2) (BD Bioscience) and anti-IL-4-BV421 (11B11) (BioLegend).

##### ACE2 transfection

Flow cytometry was utilized to determine efficiency of ACE2 transfection. Two days after transfection, HEK293T cells was harvested and washed with Hanks' balanced salt solution (HBSS, Gibco). Cells were then incubated with polyclonal rabbit anti-ACE2 (Polyclonal Rabbit IgG) (Sino Biological) in room temperature for 30 min followed by repeated washing with HBSS. Donkey anti-rabbit IgG-FITC (Ploy4064) (BioLegend) was then added to the cell suspension for extra 30 min incubation in room temperature protecting from light. Cells were then fixed with 1% formaldehyde in PBS.

##### Inhibition of receptor binding assays

HEK293T cells were transfected with a plasmid encoding human ACE2. At 48 hour post-transfection, HEK293T/ACE2 cells were collected and washed with HBSS. The RBD-His was added to the cells to a final concentration of 1 µg/ml in the presence or absence of the sera at a dilution of 1:5, followed by incubation at room temperature for 30 min. Cells were washed three times with HBSS and then incubated with anti-His Tag-PE (J095G46) (BioLegend) at room temperature for additional 30 min. After washing, cells were fixed with 1% formaldehyde in PBS.

##### Challenge of the non-human primates (Macaca mulatta) with live SARS-CoV-2

Non-human primates were immunized with two injections on day 0, day 7 via the intramuscular route with 20 µg or 40 µg per dose and then challenged with SARS-CoV-2 intranasally (0.5 ml, 10<sup>6</sup> pfu/ml) on day 28 after the first vaccination. A quantitative real-time reverse transcription-PCR (qRT-PCR) was employed to measure viral genomic RNA (gRNA) and viral subgenomic RNA (sgRNA), indicative of virus replication. Viral load in the lung tissues, throat and anal swabs, etc, were measured by qRT-PCR. The primer and probe sequences used were derived from NP gene (Forward: 5'-GGGGAACCTCTCTGCTAGAAT-3', Reverse: 5'-CAGACATTTTGCTCTCAAGCTG-3', Probe: 5'-FAMTTGCTGCTGCTTACAGATT-TAMRA-3'), according to the sequences recommended by WHO and China CDC.

SARS-CoV-2 E gene subgenomic mRNA (sgmRNA), indicative of virus replication, was assessed by RT-PCR using an approach similar to previously described<sup>33</sup>, based on The primer and probe sequences (Forward: 5'-GCTAGAGAACATCTAGACAAGAG-3', Reverse: 5'-ACACACGCATGACGACGTTATA-3', Probe: 5'-FAM-TGTGATCGGTAGGAATGACGCGAAGC-Quencher-3').

##### Adoptive therapy of splenic T cells or immune sera in the mice challenged with live SARS-CoV-2

An adoptive therapy of splenic T cells was conducted previously<sup>24,36</sup>. hACE2 mice with C57BL/6 background received 5×10<sup>7</sup>

splenic T cells isolated from either mice with same C57BL/6 background 9 days after the third dose of the candidate vaccine or from the mice treated with PBS as a control. The adoptive therapy of the sera was described previously<sup>27</sup>. The adoptive therapy based on immune sera was performed using 0.1 ml of the pooled sera from the immunized mice at the same time. In addition, hACE2 mice with ICR background received 0.8 ml sera from the mice 7 days after a single dose of the vaccine and challenged with live SARS-CoV-2. The mice were sacrificed 5 days after the challenge with live virus, and viral loads in lung tissues, lung histopathological changes, and body weight change were evaluated. Viral load in the lung tissues were measured by qRT-PCR. The primer sequences used were derived from the envelope (E) gene (Forward: 5'-TCGTTTCGGAAGAGACAGGT-3'; Reverse: 5'-GCGCAGTAAGGATGGCTAGT-3'). Sections were stained by Hematoxylin and Eosin (H&E) and evaluated under light microscopy.

Instrument

Flow cytometric data were collected using LSRFortessa (BD Biosciences) or NovoCyte (ACEA bioscience. Inc).

Software

NovoExpress 1.4.1 or FlowJo v10.0.0.

Cell population abundance

We perform the flow cytometry for phenotypes of the memory T cells with the production of IFN-gamma or IL-4 by analysing the stimulated lymphocytes in the present study, and is easy to get enough CD8+ or CD4+ cell for further gating memory cells.

Gating strategy

Cells were gated from MHC-II- and CD45R- 220-, CD4+ or CD8+ cells with CD44+ were defined as the memory cells reactive to RBD protein. From these gated cells the percentage of IL-4+ or IFN $\gamma$ + were recorded.  
ACE2 transfected-Cells with FITC fluorescence intensity were counted for the inhibition of receptor binding assays.

Tick this box to confirm that a figure exemplifying the gating strategy is provided in the Supplementary Information.